Chapter 5

Development of sulfonamide based BChE inhibitors as anti-Alzheimer's agents through scaffold hopping

5. Development of sulfonamide based BChE inhibitors as anti-Alzheimer's agents through scaffold hopping

5.1. Introduction

Scaffold hopping is a technique for obtaining new compounds by modifying the central core of an active compound. In our previous study, we developed a *piperazinedione* derivative, compound **I**, that produced significant inhibition of both AChE and BCHE enzymes [147] (**Figure 5.1**). In another study, compound **II**, a sulfonamide derivative of *para-aminobenzoic acid* (PABA), was identified as a selective inhibitor of BChE with a IC_{50} lower than compound **I** (**Figure 5.1**) [216]. Further, the compounds were permeable to BBB.

Therefore, the scaffold hopping was performed on compound **II** to obtain new compounds. In the present study, *phenylglycine*, the scaffold of compound **I** was used for substitution against the PABA of compound **II,** to obtain *N,2-diphenyl-2-(phenylsulfonamido) acetamide* (**III**) (**Figure 5.1**).

A library of sulfonamide derivatives with varying amides and esters was developed from compound **3**. A series of 22 derivatives were synthesised and characterised. The compounds were tested for AChE, BChE inhibition and cytotoxicity against SH-SY5Y was determined. The derivatives were found to be selective BChE inhibitor and BBB permeable in the *in vitro* studies. Molecular docking and MD studies were performed to identify the binding patterns of the active compounds with the BChE enzyme. The compounds displaying good inhibition on BChE were further tested on the scopolamine-induced amnesia model in rats.

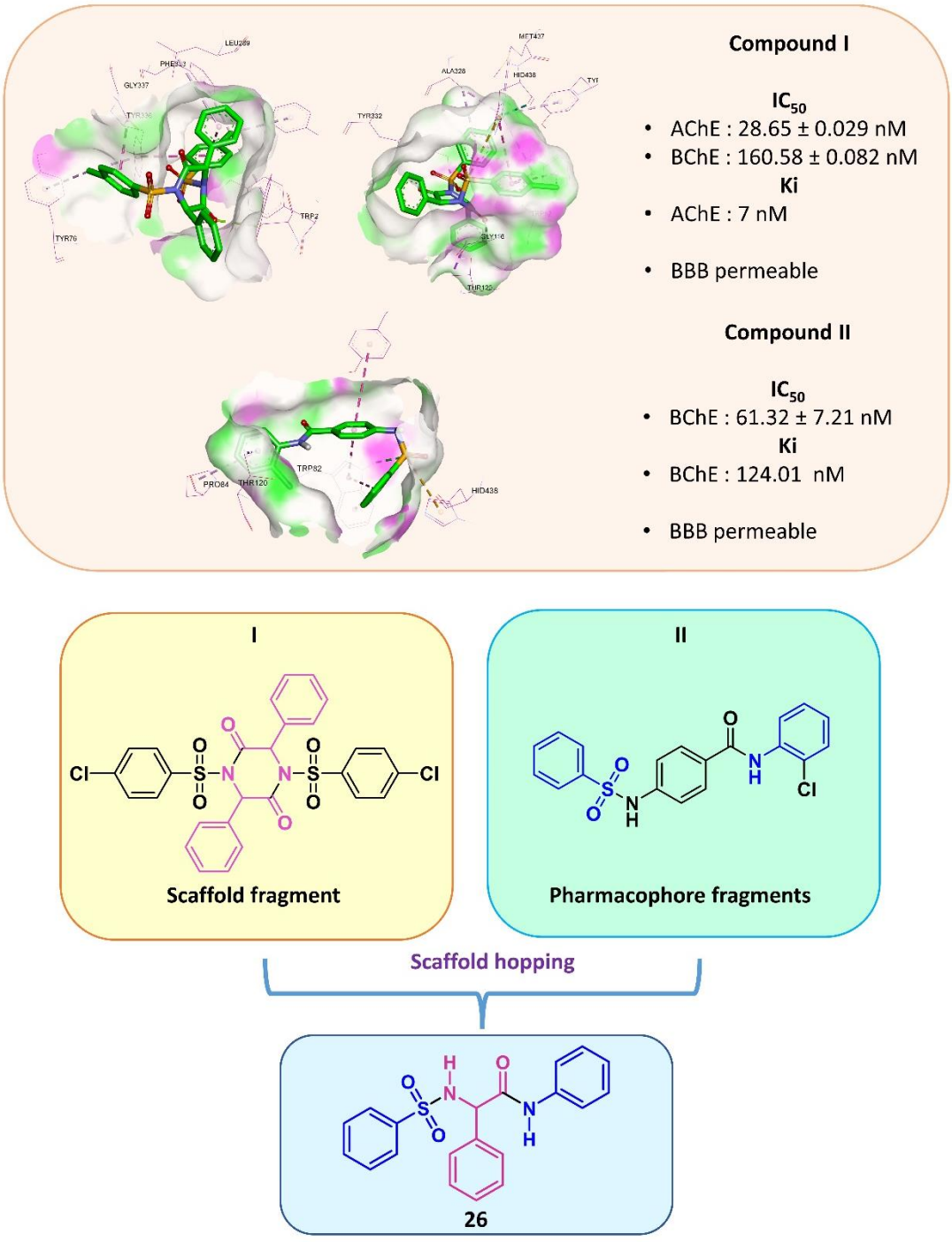

Figure 5.1 Schematic representation of the design of compound.

5.2. Materials and methods

5.2.1. Chemistry

The chemicals and solvents, of analytical grade, were purchased from Avera, Alfa Acer, Merck, Sigma Aldrich, and SD. Fine. Thin-layer chromatography (TLC), on pre-coated silica gel 60 F254 (Merck KGaA), plates were used to monitor the progress of chemical

reactions. It was visualised through ultraviolet light (254 nm) or iodine vapours. The compounds were purified by column chromatography (silica gel: 60-120 mesh size). The melting points were determined by using an automated melting point system (Barnstead Electrothermal, UK). IR(ATR) spectra were recorded on Bruker FTIR spectrometer Alpha T (Germany). The ^{1}H and ^{13}C NMR spectra were acquired in DMSO-d6 on Bruker 500 FTNMR spectrometer at operating frequencies of 500 and 125 MHz respectively. The coupling constant (*J*) was measured in Hz and the chemical shift (δ) was estimated in ppm. An UPLC/XEVO G2-XS QTOF apparatus, with APCI and ESI multi-mode ionisation sources, was used to collect mass spectra. The purity of compounds was determined by Agilent 1260 Infinity II Quaternary LC (a quaternary pump with a DAD HS G7115A detector, l ¼ 315 nm). The isocratic mobile phase was delivered by quaternary pumps with a flow rate of 1 ml/min. The mobile phase composition was phase A (acetonitrile) and phase B (methanol) in the ratio of 1:9. Further, 20 μL samples were injected into the HPLC column. The detection was made at 315 nm wavelength on SPD10AVP detector. The CLC C_{18} column (5μ, 25 cm × 4.6 mm) was used for purification. The purity of the compounds was found to be above 98%.

5.2.1.1. General procedure for the synthesis of *(S)-(+)-2-phenyl-2-(phenylsulfonamido) acetic acid* (3)

(S)-(+)-Phenylglycine (**1**) (0.0073 mole, 1 equivalent) and *sodium carbonate* (0.0219 mol, 3 equivalent) were dissolved in a mixture of 45 mL water and 15 mL acetone. One equivalent of *Benzene sulfonyl chloride* (**2**) (0.0073 mol) was diluted with 20 mL of acetone and added to the reaction mixture with continuous overnight stirring at RT. The progress of the reaction was monitored by TLC, using ethyl acetate and hexane (4:6) as the mobile phase. Acetone was evaporated from the reaction mixture after its completion under reduced pressure. It was followed by neutralisation with 1 N HCl. The crude product was filtered out, dried and recrystallised using ethanol [147, 188].

5.2.1.2. General procedure for the synthesis of substituted *(S)-(+)-N,2-diphenyl-2-(phenylsulfonamido) acetamide* (26-47)

Compound **3** (0.00086 mole, 1 equivalent) and *triethylamine* (0.0027 mole, 3 equivalent) were dissolved in 25 mL of DCM. Substituted *anilines* (1.1 equivalent) were added to the reaction mixture, followed by dropwise addition of an excess of thionyl chloride (0.00045, 5 equivalent) with continuous stirring. The mixture was stirred for 6-8 hrs, followed by evaporation of DCM under reduced pressure. The obtained residue was washed with a saturated sodium bicarbonate solution to remove compound **3** and extracted with ethyl acetate. The crude product was purified with column chromatography using ethyl acetate in hexane over silica gel (60-120 mesh) [217].

***(S)-(+)-N,2-diphenyl-2-(phenylsulfonamido) acetamide* (26)**

Brown solid (0.15 g. 47.7 % yield). M.P.: 178 – 181˚C, R_f = 0.32 (EA/Hex, 4:6, v/v). IR (ATR): 2926 (C-H stretching), 1688 (C=O stretching), 1511 (N-H stretching), 1337 (asymm. S=O stretching) and 1152 (symm. S=O stretching) cm^{-1}. ^{1}H NMR: (500 MHz, DMSO-d6) δ = 10.23 (s, 1H, CONH), 8.78 – 8.76 (d, *J* = 9.5 Hz, 1H, SO_2NH), 7.75 – 7.75 (d, *J* = 7 Hz, 2H, Ar-H), 7.48 – 7.45 (t, *J* = 4 Hz, 1H, Ar-H), 7.42 – 7.37 (m, 5H, Ar-H), 7.27 – 7.21 (m, 4H, Ar-H), 7.03 – 7.01 (t, *J* = 5 Hz, 1H, Ar-H), 5.20 – 5.18 (d, *J* = 9.5 Hz, 1H, CH). ^{13}C NMR (125 MHz, DMSO-d6): δ = 167.37, 140.86, 138.19, 137.01, 132.06, 128.60, 128.20, 127.70, 126.93, 126.36, 123.60, 119.16, 60.00. MS (EI+): m/z calculated for $C_{20}H_{18}N_2O_3S$ 366.44, found – 366.46 (M^+).

***(S)-(+)-N-(2-fluorophenyl)-2-phenyl-2-(phenylsulfonamido) acetamide* (27)**

Brown solid (0.305 g, 92.45 % yield). M.P.: 169 – 172˚C, R_f = 0.43 (EA/Hex, 4:6, v/v). IR (ATR): 3251 (secondary NH stretching), 2977 (C-H stretching), 1694 (C=O stretching), 1533 (N-H stretching), 1347 (asymm. S=O stretching) and 1167 (symm. S=O stretching) cm^{-1}. ^{1}H NMR: (500 MHz, DMSO-d6) δ = 10.07 (s, 1H, CONH), 8.78 – 8.76 (d, *J* = 9.6 Hz, 1H, SO_2NH), 7.78 – 7.76 (d, *J* = 7.7 Hz, 2H, Ar-H), 7.49 – 7.39 (m, 6H,

Ar-H), 7.29 – 7.21 (m, 6H, Ar-H), 5.44 – 5.42 (d, *J* = 9.1 Hz, 1H, CH). ^{13}C NMR: (125 MHz, DMSO-d6) δ = 168.62, 141.50, 141.41, 137.58, 132.68, 132.26, 129.39, 128.81, 128.38, 127.59, 126.98, 126.90, 121.80, 119.60, 60.02. MS (EI+): m/z calculated for $C_{20}H_{17}FN_2O_3S$ 384.43, found – 384.47 (M^+).

***(S)-(+)-N-(3-fluorophenyl)-2-phenyl-2-(phenylsulfonamido) acetamide* (28)**

Brown solid (0.191 g, 57.89 % yield). M.P.: 173 – 175˚C, R_f = 0.37 (EA/Hex, 4:6, v/v). IR (ATR): 3245 (secondary NH stretching), 2977 (C-H stretching), 1694 (C=O stretching), 1510 (N-H stretching), 1337 (asymm. S=O stretching) and 1147 (symm. S=O stretching) cm^{-1}. ^{1}H NMR: (500 MHz, DMSO-d6) *δ* = 10.03 (s, 1H, CONH), 8.75 – 8.73 (d, *J* = 9.5 Hz, 1H, SO_2NH), 7.73 – 7.71 (d, *J* = 7.6 Hz, 2H, Ar-H), 7.48 – 7.39 (m, 6H, Ar-H), 7.29 – 7.22 (m, 6H, Ar-H), 5.44 – 5.42 (d, *J* = 9.3 Hz, 1H, CH). ^{13}C NMR: (125 MHz, DMSO-d6) *δ* = 168.62, 143.26, 139.97, 132.69, 129.27, 128.81, 128.28, 127.83, 127.74, 127.42, 126.90, 125.01, 121.80, 119.59, 60.02. MS (EI+): m/z calculated for $C_{20}H_{17}FN_2O_3S$ 384.43, found – 384.48 (M^+).

***(S)-(+)-N-(4-fluorophenyl)-2-phenyl-2-(phenylsulfonamido) acetamide* (29)**

Pale brown solid (0.24 g, 84.87 % yield). M.P.: 175 – 179˚C, R_f = 0.39 (EA/Hex, 4:6, v/v). IR (ATR): 3267 (secondary NH stretching), 2921 (C-H stretching), 1683 (C=O stretching), 1505 (N-H stretching), 1344 (asymm. S=O stretching) and 1166 (symm. S=O stretching) cm^{-1}. ^{1}H NMR: (500 MHz, DMSO-d6) δ = 10.36 (s, 1H, CONH), 8.83 – 8.81 (d, *J* = 9.5 Hz, 1H, SO_2NH), 7.81 – 7.79 (d, *J* = 7.4 Hz, 2H, Ar-H), 7.46 – 7.35 (m, 6H, Ar-H), 7.26 – 7.18 (m, 4H, Ar-H), 7.09 – 7.01 (m, 2H, Ar-H), 5.16 – 5.14 (d, *J* = 9.5 Hz, 1H, CH). ^{13}C NMR: (125 MHz, DMSO-d6) δ = 167.86, 159.63, 157.71, 141.36, 137.45, 135.12, 132.66, 129.17, 128.80, 128.32, 127.50, 126.96, 121.56, 121.50, 115.86, 115.69, 60.57. MS (EI+): m/z calculated for $C_{20}H_{17}FN_2O_3S$ 384.43, found – 384.48 (M^+).

***(S)-(+)-N-(2-chlorophenyl)-2-phenyl-2-(phenylsulfonamido) acetamide* (30)**

Pale brown solid (0.173 g, 50.28 % yield). M.P.:148 – 158˚C, R_f = 0.51 (EA/Hex, 4:6, v/v). IR (ATR): 3240 (secondary NH stretching), 2975 (C-H stretching), 1694 (C=O stretching), 1510 (N-H stretching), 1337 (asymm. S=O stretching) and 1146 (symm. S=O stretching) cm^{-1}. ^1H NMR: (500 MHz, DMSO-d6) δ = 9.87 (s, 1H, CONH), 8.81 – 8.79 (d, *J* = 9.6 Hz, 1H, SO_2NH), 7.81 -7.79 (d, *J* = 7.7 Hz, 2H, Ar-H), 7.55 – 7.53 (d, *J* = 7.2 Hz, 1H, Ar-H), 7.49 – 7.42 (m, 5H, Ar-H), 7.32 – 7.23 (m, 5H, Ar-H), 7.17 – 7.14 (t, *J* = 7.6 Hz, 1H, Ar-H), 5.44 – 4.42 (d, *J* = 9.4 Hz, 1H, CH). ^{13}C NMR: (125 MHz, DMSO-d6) δ = 168.57, 141.43, 137.59, 134.44, 132.75, 129.93, 129.39, 129.31, 128.72, 128.27, 127.79, 127.63, 127.05, 126.76, 126.19, 126.03, 60.03. MS (EI+): m/z calculated for $C_{20}H_{17}ClN_2O_3S$ 400.88, found – 400.95, 402.96 [M^+, M^{+2} (3:1)].

***(S)-(+)-N-(3-chlorophenyl)-2-phenyl-2-(phenylsulfonamido) acetamide* (31)**

Pale brown solid (0.166 g, 48.25 % yield). M.P.: 173 – 177˚C, R_f = 0.45 (EA/Hex, 4:6, v/v). IR (ATR): 3268 (secondary NH stretching), 2954 (C-H stretching), 1658 (C=O stretching), 1532 (N-H stretching), 1345 (asymm. S=O stretching) and 1165 (symm. S=O stretching) cm^{-1}. ^1H NMR: (500 MHz, DMSO-d6) δ = 10.34 (s, 1H, CONH), 8.81 – 8.79 (d, *J* = 9.5 Hz, 1H, SO_2NH), 7.74 – 7.72 (d, *J* = 7.4 Hz, 2H, Ar-H), 7.48 – 7.36 (m, 6H, Ar-H), 7.32 – 7.30 (d, *J* = 8.8 Hz, 1H, Ar-H), 7.28 – 7.22 (m, 5H, Ar-H), 5.16 – 5.14 (d, *J* = 9.5 Hz, 1H, CH). ^{13}C NMR: (125 MHz, DMSO-d6) δ = 167.27, 141.22, 140.11, 137.12, 133.41, 132.75, 130.92, 129.20, 128.87, 127.53, 126.91, 125.90, 123.93, 119.23, 118.07, 107.40, 60.56. MS (EI+): m/z calculated for $C_{20}H_{17}ClN_2O_3S$ 400.88, found – 400.93, 402.98 [M^+, M^{+2} (3:1)].

***(S)-(+)-N-(4-chlorophenyl)-2-phenyl-2-(phenylsulfonamido) acetamide* (32)**

Pale brown solid (0.192 g, 55.81 % yield). M.P.:179 – 183˚C, R_f = 0.39 (EA/Hex, 4:6, v/v). IR (ATR): 3258 (secondary NH stretching), 2977 (C-H stretching), 1686 (C=O stretching), 1555 (N-H stretching), 1336 (asymm. S=O stretching) and 1151 (symm. S=O stretching) cm^{-1}. ^1H NMR: (500 MHz, DMSO-d6) δ = 10.38 (s, 1H, CONH), 8.81 – 8.79

(d, *J* = 9.5 Hz, 1H, SO_2NH), 7.75 – 7.73 (d, *J* = 7.4 Hz, 2H, Ar-H), 7.48 – 7.45 (m, 1H, Ar-H), 7.42 – 7.36 (m, 7H, Ar-H), 7.32 – 7.30 (d, *J* = 8.8 Hz, 2H, Ar-H), 7.27 – 7.22 (m, 3H, Ar-H), 5.18 – 5.16 (d, *J* = 9.5 Hz, 1H, CH). ^{13}C NMR: (125 MHz, DMSO-d6) δ = 167.52, 140.75, 137.11, 136.74, 132.11, 128.61, 128.54, 128.26, 127.80, 127.21, 126.94, 126.38, 120.73, 60.04. MS (EI+): m/z calculated for $C_{20}H_{17}ClN_2O_3S$ 400.88, found – 401.07, 403.06 [M^+, M^{+2} (3:1)]

***(S)-(+)-N-(2-bromophenyl)-2-phenyl-2-(phenylsulfonamido) acetamide* (33)**

Pale brown solid (0.232 g, 60.70 % yield). M.P.:165 – 168˚C, R_f = 0.49 (EA/Hex, 4:6, v/v). IR (ATR): 3258 (secondary NH stretching), 2977 (C-H stretching), 1686 (C=O stretching), 1555 (N-H stretching), 1336 (asymm. S=O stretching) and 1151 (symm. S=O stretching) cm^{-1}. ^{1}H NMR: (500 MHz, DMSO-d6) δ = 10.38 (s, 1H, CONH), 8.81 – 8.79 (d, *J* = 9.5 Hz, 1H, SO_2NH), 7.75 – 7.73 (d, *J* = 7.4 Hz, 2H, Ar-H), 7.48 – 7.45 (m, 1H, Ar-H), 7.42 – 7.36 (m, 7H, Ar-H), 7.32 – 7.30 (d, *J* = 8.8 Hz, 2H, Ar-H), 7.27 – 7.22 (m, 3H, Ar-H), 5.18 – 5.16 (d, *J* = 9.5 Hz, 1H, CH). ^{13}C NMR: (125 MHz, DMSO-d6) δ 167.52, 140.75, 137.11, 136.74, 132.11, 128.61, 128.54, 128.26, 127.80, 127.21, 126.94, 126.38, 120.73, 60.04. MS (EI+): m/z calculated for $C_{20}H_{17}BrN_2O_3S$ 445.33, found – 445.39, 447.01 [M^+, M^{+2} (1:1)].

***(S)-(+)-N-(3-bromophenyl)-2-phenyl-2-(phenylsulfonamido) acetamide* (34)**

Brown solid (0.212 g, 55.47 % yield). M.P.: 174 – 178˚C, R_f = 0.43 (EA/Hex, 4:6, v/v). IR (ATR): 3269 (secondary NH stretching), 2978 (C-H stretching), 1694 (C=O stretching), 1530 (N-H stretching), 1346 (asymm. S=O stretching) and 1166 (symm. S=O stretching) cm^{-1}. ^{1}H NMR (500 MHz, DMSO-d6) δ =10.42 (s, 1H, CONH), 8.82 – 8.80 (d, *J* = 9.4 Hz, 1H, SO_2NH), 7.76 – 7.74 (d, *J* = 7.4 Hz, 2H, Ar-H), 7.69 (s, 1H, Ar-H), 7.50 – 7.47 (t, *J* = 7.5 Hz, 1H, Ar-H), 7.43 – 7.36 (m, 4H, Ar-H), 7.25 (m, 6H, Ar-H), 5.16 – 5.14 (d, *J* = 9.4 Hz, 1H, CH). ^{13}C NMR (125 MHz, DMSO-d6) δ =168.28, 141.28, 140.24, 137.16, 132.69, 131.23, 129.21, 128.87, 128.44, 127.53, 126.98, 126.85, 122.11,

121.92, 118.53, 60.64. MS (EI+): m/z calculated for $C_{20}H_{17}BrN_2O_3S$ 445.33, found – 445.37, 447.02 [M^+, M^{+2} (1:1)].

***(S)-(+)-N-(4-bromophenyl)-2-phenyl-2-(phenylsulfonamido) acetamide* (35)**

Brown solid (0.256 g, 66.98 % yield). M.P.: 185 – 189˚C, R_f = 0.4 (EA/Hex, 4:6, v/v). IR (ATR): 3255 (secondary NH stretching), 2978 (C-H stretching), 1655 (C=O stretching), 1527 (N-H stretching), 1349 (asymm. S=O stretching) and 1167 (symm. S=O stretching) cm^{-1}. ^{1}H NMR: (500 MHz, DMSO-d6) δ =10.38 (s, 1H, CONH), 8.82 – 8.80 (d, *J* = 9.5 Hz, 1H, SO_2NH), 7.75 – 7.74 (d, *J* = 7.4 Hz, 2H, Ar-H), 7.48 – 7.40 (m, 5H, Ar-H), 7.37 – 7.35 (m, 4H, Ar-H), 7.29 – 7.23 (m, 3H, Ar-H), 5.18 – 5.16 (d, *J* = 9.5 Hz, 1H, CH). ^{13}C NMR: (125 MHz, DMSO-d6) δ =167.53, 140.74, 137.52, 136.71, 132.12, 131.44, 128.61, 128.26, 127.80, 126.94, 126.38, 121.10, 115.26, 60.05. MS (EI+): m/z calculated for $C_{20}H_{17}BrN_2O_3S$ 445.33, found – 445.35, 447.01 [M^+, M^{+2} (1:1)].

***(S)-(+)-N-(2-methoxyphenyl)-2-phenyl-2-(phenylsulfonamido) acetamide* (36)**

Buff solid (0.210 g, 61.72 % yield). M.P.: 155 – 159˚C, R_f = 0.4 (EA/Hex, 4:6, v/v). IR (ATR): 3245 (secondary NH stretching), 2975 (C-H stretching), 1694 (C=O stretching), 1510 (N-H stretching), 1337 (asymm. S=O stretching) and 1146 (symm. S=O stretching) cm^{-1}. ^{1}H NMR: (500 MHz, DMSO-d6) δ =9.53 (s, 1H, CONH), 8.72 – 8.74 (d, *J* = 9.4 Hz, 1H, SO_2NH), 7.78 – 7.76 (d, *J* = 7.4 Hz, 2H, Ar-H), 7.66 – 7.64 (d, *J* = 10 Hz, 1H, Ar-H), 7.52 – 7.49 (d, *J* = 7.4 Hz, 1H, Ar-H), 7.45 – 7.42 (t, *J* = 7.6 Hz, 2H, Ar-H), 7.38 – 7.37 (d, *J* = 6.9 Hz, 2H, Ar-H), 7.26 – 7.20 (m, 3H, Ar-H), 7.07 – 7.00 (m, 2H, Ar-H), 6.85 – 6.82 (m, 1H, Ar-H), 5.48 – 5.46 (d, *J* = 9.4 Hz, 1H, CH), 3.80 (s, 3H, CH_3). ^{13}C NMR: (125 MHz, DMSO-d6) δ =167.74, 149.47, 140.87, 137.29, 132.06, 128.62, 128.04, 127.53, 127.15, 126.40, 124.64, 121.46, 120.03, 111.13, 59.60, 55.65. MS (EI+): m/z calculated for $C_{21}H_{20}N_2O_4S$ 396.46, found – 396.55 (M^+).

***(S)-(+)-N-(3-methoxyphenyl)-2-phenyl-2-(phenylsulfonamido) acetamide* (37)**

Buff solid (0.242 g, 71.12 % yield). M.P.: 161 – 164˚C, R_f = 0.4 (EA/Hex, 4:6, v/v). IR (ATR): 3252 (secondary NH stretching), 2920 (C-H stretching), 1653 (C=O stretching), 1530 (N-H stretching), 1342 (asymm. S=O stretching) and 1162 (symm. S=O stretching) cm^{-1}. ^{1}H NMR: (500 MHz, DMSO-d6) δ =10.23 (s, 1H, CONH), 8.78 – 8.76 (d, *J* = 9.5 Hz, 1H, SO_2NH), 7.76 – 7.74 (d, *J* = 7.5 Hz, 2H, Ar-H), 7.49 – 7.46 (t, *J* = 7.3 Hz, 1H, Ar-H), 7.43 – 7.37 (m, 4H, Ar-H), 7.27 – 7.21 (m, 3H, Ar-H), 7.17 – 7.14 (t, *J* = 8.2 Hz, 1H, Ar-H), 7.08 (s, 1H, Ar-H), 6.95 – 6.94 (d, *J* = 8.0 Hz, 1H, Ar-H), 6.62 – 6.60 (dd, *J* = 8.2, 2.2 Hz, 1H), 5.19 – 5.17 (d, *J* = 9.4 Hz, 1H, CH), 3.69 (s, 3H, CH_3). ^{13}C NMR: (125 MHz, DMSO-d6) δ =167.40, 159.30, 140.84, 139.36, 136.94, 132.06, 129.42, 128.59, 128.20, 127.72, 126.94, 126.36, 111.39, 109.10, 104.89, 60.06, 54.85. MS (EI+): m/z calculated for $C_{21}H_{20}N_2O_4S$ 396.46, found – 396.49 (M^+).

***(S)-(+)-N-(4-methoxyphenyl)-2-phenyl-2-(phenylsulfonamido) acetamide* (38)**

Buff solid (0.179 g, 52.61 % yield). M.P.: 174 – 178˚C, R_f = 0.36 (EA/Hex, 4:6, v/v). IR (ATR): 3254 (secondary NH stretching), 2921 (C-H stretching), 1683 (C=O stretching), 1520 (N-H stretching), 1342 (asymm. S=O stretching) and 1152 (symm. S=O stretching) cm^{-1}. ^{1}H NMR: (500 MHz, DMSO-d6) δ = 10.10 (s, 1H, CONH), 8.74 – 8.72 (d, *J* = 9.6 Hz, 1H, SO_2NH), 7.75 – 7.74 (d, *J* = 7.4 Hz, 2H, Ar-H), 7.50 – 7.47 (t, *J* = 7.4 Hz, 1H, Ar-H), 7.43 – 7.36 (m, 5H, Ar-H), 7.29 – 7.20 (m, 6H, Ar-H), 6.83 – 6.81 (d, *J* = 9.0 Hz, 2H, Ar-H), 5.16 – 5.14 (d, *J* = 9.6 Hz, 1H, CH), 3.69 (s, 3H, OCH_3). ^{13}C NMR: (125 MHz, DMSO-d6) δ = 167.44, 155.97, 141.44, 137.74, 132.62, 131.83, 129.16, 128.73, 128.21, 127.47, 126.94, 121.32, 114.29, 60.52, 55.62. MS (EI+): m/z calculated for $C_{21}H_{20}N_2O_4S$ 396.46, found – 396.48 (M^+).

***(S)-(+)-N-(3-nitrophenyl)-2-phenyl-2-(phenylsulfonamido) acetamide* (39)**

Brown solid (0.3 g, 84.96 % yield). M.P.: 183 – 187˚C, R_f = 0.31 (EA/Hex, 4:6, v/v). IR (ATR): 3252 (secondary NH stretching), 2978 (C-H stretching), 1695 (C=O stretching),

1510 (N-H stretching), 1337 (asymm. S=O stretching) and 1148 (symm. S=O stretching) cm^{-1}. ^{1}H NMR: (500 MHz, DMSO-d6) δ = 10.75 (s, 1H, CONH), 8.88 – 8.86 (d, *J* = 9.2 Hz, 1H, SO_2NH), 7.77 – 7.75 (d, *J* = 7.3 Hz, 2H, Ar-H), 7.48 – 7.44 (m, 2H, Ar-H), 7.43 – 7.38 (m, 6H, Ar-H), 7.29 – 7.22 (m, 4H, Ar-H), 5.18 – 5.16 (d, *J* = 9.3 Hz, 1H, CH). ^{13}C NMR: (125 MHz, DMSO-d6) δ = 168.76, 141.50, 138.82, 136.96, 133.14, 132.69, 129.27, 128.81, 128.70, 128.28, 127.70, 126.90, 125.00, 119.59, 110.07, 60.02. MS (EI+): m/z calculated for $C_{21}H_{20}N_2O_4S$ 411.43, found – 411.45 (M^+).

***(S)-(+)-N-(4-nitrophenyl)-2-phenyl-2-(phenylsulfonamido) acetamide* (40)**

Brown solid (0.310 g, 87.70 % yield). M.P.: 185 – 189˚C, R_f = 0.31 (EA/Hex, 4:6, v/v). IR (ATR): 3275 (secondary NH stretching), 2921 (C-H stretching), 1710 (C=O stretching), 1546 (N-H stretching), 1336 (asymm. S=O stretching) and 1158 (symm. S=O stretching) cm^{-1}. ^{1}H NMR: (500 MHz, DMSO-d6) δ = 10.72 (s, 1H, CONH), 8.75 – 8.73 (d, *J* = 9.3 Hz, 1H, SO_2NH), 8.00 – 7.98 (d, *J* = 8.4 Hz, 2H, Ar-H), 7.73 – 7.72 (d, *J* = 8.1 Hz, 2H, Ar-H), 7.56 – 7.52 (m, 3H, Ar-H), 7.47 – 7.40 (m, 4H, Ar-H), 7.27 – 7.25 (m, 3H, Ar-H), 4.92 – 4.90 (d, *J* = 9.3 Hz, 1H, CH). ^{13}C NMR: (125 MHz, DMSO-d6) δ = 170.84, 140.95, 136.40, 132.11, 128.70, 128.24, 127.81, 127.72, 127.28, 127.18, 126.34, 124.40, 119.09, 109.48, 59.45. MS (EI+): m/z calculated for $C_{21}H_{20}N_2O_4S$ 411.43, found – 411.44 (M^+).

***(S)-(+)-N-(2-methylphenyl)-2-phenyl-2-(phenylsulfonamido) acetamide* (41)**

Pale-yellow solid (0.301 g, 92.19 % yield). M.P.: 171 – 174˚C, R_f = 0.46 (EA/Hex, 4:6, v/v). IR (ATR): 3258 (secondary NH stretching), 2954 (C-H stretching), 1696 (C=O stretching), 1547 (N-H stretching), 1335 (asymm. S=O stretching) and 1155 (symm. S=O stretching) cm^{-1}. ^{1}H NMR: (500 MHz, DMSO-d6) δ = 9.62 (s, 1H, CONH), 8.77 – 8.55 (d, *J* = 9.6 Hz, 1H, SO_2NH), 7.81 – 7.79 (d, *J* = 7.9 Hz, 2H, Ar-H), 7.50 – 7.47 (m, 2H, Ar-H), 7.44 – 7.40 (m, 4H, Ar-H), 7.30 – 7.24 (m, 4H, Ar-H), 7.06 – 6.99 (m, 2H, Ar-H), 5.32 – 5.30 (d, *J* = 9.4 Hz, 1H, Ar-H), 1.91 (s, 3H, CH_3). ^{13}C NMR: (125 MHz, DMSO-

d6) δ = 168.17, 141.54, 138.08, 135.73, 132.28, 129.30, 128.72, 128.28, 128.21, 127.47, 127.01, 126.35, 125.41, 119.60, 110.06, 60.11, 17.81. MS (EI+): m/z calculated for $C_{21}H_{20}N_2O_3S$ 380.46, found – 380.47 (M^+).

***(S)-(+)-N-(3-methylphenyl)-2-phenyl-2-(phenylsulfonamido) acetamide* (42)**

Pale-yellow solid (0.289 g, 88.51 % yield). M.P.: 172 – 175˚C, R_f = 0.45 (EA/Hex, 4:6, v/v). IR (ATR): 3258 (secondary NH stretching), 2924 (C-H stretching), 1654 (C=O stretching), 1539 (N-H stretching), 1344 (asymm. S=O stretching) and 1166 (symm. S=O stretching) cm^{-1}. ^{1}H NMR: (500 MHz, DMSO-d6) δ = 10.15 (s, 1H, CONH), 8.76 – 8.74 (d, *J* = 9.5 Hz, 1H, SO_2NH), 7.76 – 7.74 (d, *J* = 7.2 Hz, 2H, Ar-H), 7.50 – 7.47 (t, *J* = 7.4 Hz, 1H, Ar-H), 7.43 – 7.37 (m, 4H, Ar-H), 7.27 – 7.11 (m, 6H, Ar-H), 6.86 – 6.84 (d, J = 10 Hz, 1H, Ar-H), 5.19 – 5.17 (d, *J* = 9.5 Hz, 1H, CH), 2.23 (s, 3H, CH_3). ^{13}C NMR: (125 MHz, DMSO-d6) δ = 167.30, 140.87, 138.10, 137.81, 137.05, 132.05, 128.61, 128.43, 128.18, 127.68, 126.93, 126.36, 124.29, 119.74, 116.38, 59.99, 20.97. MS (EI+): m/z calculated for $C_{21}H_{20}N_2O_3S$ 380.46, found – 380.49 (M^+).

***(S)-(+)-N-(4-methylphenyl)-2-phenyl-2-(phenylsulfonamido) acetamide* (43)**

Pale-yellow solid (0.309 g, 94.90 % yield). M.P.: 174 – 177˚C, R_f = 0.44 (EA/Hex, 4:6, v/v). IR (ATR): 3250 (secondary NH stretching), 2920 (C-H stretching), 1695 (C=O stretching), 1528 (N-H stretching), 1342 (asymm. S=O stretching) and 1161 (symm. S=O stretching) cm^{-1}. ^{1}H NMR (500 MHz, DMSO-d6) δ = 10.14 (s, 1H, CONH), 8.76 – 8.74 (d, *J* = 9.6 Hz, 1H, SO_2NH), 7.75 - 7.74 (d, *J* = 7.1 Hz, 2H, Ar-H), 7.50 – 7.46 (m, 1H, Ar-H), 7.42 – 7.37 (m, 4H, Ar-H), 7.27 – 7.22 (m, 5H, Ar-H), 7.06 – 7.06 (d, *J* = 8.2 Hz, 2H, Ar-H), 5.19 – 5.17 (d, *J* = 9.6 Hz, 1H, CH), 2.22 (s, 2H, CH_3). ^{13}C NMR (125 MHz, DMSO-d6) δ = 167.11, 140.86, 137.10, 135.66, 132.55, 132.04, 128.95, 128.93, 128.58, 128.56, 128.16, 128.14, 127.65, 126.91, 126.89, 126.35, 126.33, 119.20, 119.18, 59.97, 20.31. MS (EI+): m/z calculated for $C_{21}H_{20}N_2O_3S$ 380.46, found – 380.49 (M^+).

***(S)-(+)-N-(2-ethylphenyl)-2-phenyl-2-(phenylsulfonamido) acetamide* (44)**

Pale-yellow solid (0.160 g, 47.25 % yield). M.P.: 179 – 183˚C, R_f = 0.42 (EA/Hex, 4:6, v/v). IR (ATR): 3259 (secondary NH stretching), 2920 (C-H stretching), 1694 (C=O stretching), 1522 (N-H stretching), 1343 (asymm. S=O stretching) and 1162 (symm. S=O stretching) cm^{-1}. ^{1}H NMR: (500 MHz, DMSO-d6) δ = 9.58 (s, 1H, CONH), 8.76-8.74 (d, *J* = 9.4 Hz, 1H, SO_2NH), 7.81 – 7.79 (d, *J* = 7.3 Hz, 2H, Ar-H), 7.57 – 7.55 (m, 1H, Ar-H), 7.49 – 7.42 (t, *J* = 7.6 Hz, 2H, Ar-H), 7.44 – 7.42 (d, *J* = 7.2 Hz, 2H, Ar-H), 7.30 – 7.23 (m, 3H, Ar-H), 7.15 – 7.08 (m, 3H, Ar-H), 6.95 – 6.93 (m, 1H, Ar-H), 5.32 – 5.30 (d, *J* = 9.4 Hz, 1H), 2.34 – 2.20 (m, 1H, CH_2), 0.82 – 0.79 (t, *J* = 7.5 Hz, 1H, CH_3). ^{13}C NMR: (125 MHz, DMSO-d6) δ = 168.44, 141.58, 138.57, 138.05, 135.03, 132.70, 129.29, 129.09, 128.68, 128.19, 127.49, 127.01, 126.48, 126.34, 126.27, 60.10, 23.98, 14.65. MS (EI+): m/z calculated for $C_{21}H_{20}N_2O_3S$ 394.49, found – 394.51 (M^+).

***(S)-(+)-O-methyl 2-phenyl-2-(phenylsulfonamido) acetate* (45)**

White solid (0.230 g, 87.77 % yield). M.P.: 163 – 168˚C, R_f = 0.52 (EA/Hex, 4:6, v/v). IR (ATR): 3283 (secondary NH stretching), 2920 (C-H stretching), 1744 (C=O stretching), 1553 (N-H stretching), 1333 (asymm. S=O stretching) and 1159 (symm. S=O stretching) cm^{-1}. ^{1}H NMR: (500 MHz, DMSO DMSO-d6) δ = 8.93 – 8.91 (d, *J* = 7.9 Hz, 1H, SO_2NH), 7.74 – 7.72 (d, *J* = 7.2 Hz, 2H, Ar-H), 7.59 – 7.56 (t, *J* = 10.5, 4.3 Hz, 1H, Ar-H), 7.51 – 7.48 (t, *J* = 7.6 Hz, 2H, Ar-H), 7.27 (s, 5H), 5.05 – 5.03 (d, *J* = 8.0 Hz, 1H, CH), 3.44 (s, 3H, OCH_3). ^{13}C NMR: (125 MHz, DMSO-d6) δ = 169.96, 140.66, 135.51, 132.26, 128.79, 128.41, 128.14, 127.20, 126.35, 59.30, 52.20. MS (EI+): m/z calculated for $C_{22}H_{22}N_2O_3S$ 305.35, found – 305.41 (M^+).

***(S)-(+)-O-ethyl 2-phenyl-2-(phenylsulfonamido) acetate* (46)**

Off-white solid (0.262 g, 95.59 % yield). M.P.: 173 – 176˚C, R_f = 0.51 (EA/Hex, 4:6, v/v). IR (ATR): 3250 (secondary NH stretching), 2978 (C-H stretching), 1706 (C=O stretching), 1528 (N-H stretching), 1331 (asymm. S=O stretching) and 1164 (symm. S=O

stretching) cm^{-1}. ^{1}H NMR (500 MHz, DMSO-d6) δ = 8.92 – 8.90 (d, *J* = 6.8 Hz, 1H, SO_2NH), 7.76 – 7.74 (d, *J* = 7.6 Hz, 2H, Ar-H), 7.59 – 7.48 (m, 3H, Ar-H), 7.28 (s, 5H, Ar-H), 5.01 – 5.00 (d, *J* = 7.1 Hz, 1H, CH), 3.95 – 3.83 (m, 2H, CH_2), 1.01 – 0.97 (t, *J* = 7.1 Hz, 3H, CH_3). ^{13}C NMR (125 MHz, DMSO-d6) δ = 169.44, 140.73, 135.65, 132.27, 128.80, 128.41, 128.11, 127.16, 126.38, 61.02, 59.37, 13.61. MS (EI+): m/z calculated for $C_{22}H_{22}N_2O_3S$ 319.38, found – 319.41 (M^+).

***(S)-(+)-O-butyl 2-phenyl-2-(phenylsulfonamido) acetate* (47)**

Off-white solid (0.256 g,85.86 % yield). M.P.: 177 – 180˚C, R_f = 0.51 (EA/Hex, 4:6, v/v). IR (ATR): 3286 (secondary NH stretching), 2961 (C-H stretching), 1725 (C=O stretching), 1531 (N-H stretching), 1334 (asymm. S=O stretching) and 1161(symm. S=O stretching) cm^{-1}. ^{1}H NMR: (500 MHz, DMSO-d6) δ = 8.92 – 8.90 (d, *J* = 9.4 Hz, 1H, SO_2NH), 7.75 – 7.74 (d, *J* = 7.5 Hz, 2H, Ar-H), 7.59 – 7.56 (t, *J* = 7.3 Hz, 1H, Ar-H), 7.51 – 7.48 (t, *J* = 7.7 Hz, 2H, Ar-H), 7.27 (s, 5H, Ar-H), 5.02 – 5.00 (d, *J* = 9.4 Hz, 1H, CH), 3.89 – 3.80 (qd, *J* = 10.9, 5.5 Hz, 2H, CH_2), 1.38 – 1.32 (m, *J* = 13.2, 6.4 Hz, 2H, CH_2), 1.14 – 1.09 (dd, *J* = 15.0, 7.5 Hz, 2H, CH_2), 0.76 (t, *J* = 7.4 Hz, 3H, CH_3). ^{13}C NMR: (125 MHz, DMSO-d6) δ = 170.06, 141.29, 136.28, 132.83, 129.37, 128.95, 128.67, 127.70, 126.92, 65.17, 59.96, 30.28, 18.72, 13.85. MS (EI+): m/z calculated for $C_{22}H_{22}N_2O_3S$ 347.43, found – 347.44 (M^+).

5.2.2. *In vitro* ChE inhibitory activity

The *in vitro* ChE inhibition assay was performed in a similar manner as reported in section 4.2.3. The IC_{50} value of the compounds was determined using seven different concentrations of inhibitor, i.e., 0.1, 1, 10, 50, 75, 100 and 200 µM prepared in methanol. Five different concentrations, i.e., 3, 6, 9, 12 and 15 µM of compound **30** and 4, 8, 12, 16 and 20 µM of compound **33,** were used for determining the kinetics of enzyme inhibition.

5.2.3. *In vitro* blood-brain barrier permeation assay

The *in vitro* BBB permeation assay was performed in a similar manner as reported in section 4.2.4.

5.2.4. Cell viability (MTT Assay)

The *in vitro* cell viability assay was performed in a similar manner as reported in section 4.2.5.

5.2.5. *In silico* ADMET and molecular property analysis

The *in silico* ADMET study was performed as reported in section 4.2.6.

5.2.6. Molecular docking

The molecular docking was performed using the protocol reported in section 4.2.7.

5.2.7. Molecular dynamics

The MD was performed using the protocol reported in section 4.2.9.

5.2.8. *In vivo* evaluation of compounds

5.2.8.1. Drugs and treatments

The animals were housed by following protocol reported in section 4.2.10.1. Scopolamine hydrobromide (SCO) was used to induced amnesia at a dose of 5 mg/Kg. The animals were divided into nine groups, each containing six animals. The following treatments was used in the study: (I) control, (II) SCO (5 mg/Kg), (III) SCO + donepezil (5 mg/Kg), (IV) SCO + compound **30** (5 mg/Kg), (V) SCO + compound **30** (10 mg/Kg), (VI) SCO + compound **30** (20 mg/Kg), (VII) SCO + compound **33** (5 mg/Kg), (VIII) SCO + compound **33** (10 mg/Kg), and (IX) SCO + compound **33** (20 mg/Kg). Donepezil and SCO were freshly dissolved in the distilled water and investigational compounds were suspended in 0.5% SCMC just before the dosing. SCO was administered through intraperitoneal injection (i.p.), while other compounds were administered through oral route (p.o.) by using oral gavage. The compounds were administered for seven days, while

SCO was administered only on the seventh day to induce amnesia. The behavioural test were carried out after half an hour of the administration of SCO [204].

5.2.8.2. LD_{50} determination

The LD_{50} was determined using the protocol reported in section 4.2.10.2. The complete data related to LD_{50} of the compounds is reported in appendix (**Table T14 – T25**).

5.2.8.3. Y-maze test

The Y-maze test was carried out using the protocol reported in section 4.2.10.3.

5.2.8.4. Barnes maze

The Barnes maze test was carried out using the protocol reported in section 4.2.10.4.

5.2.8.5. Neurochemical analysis

The neurochemical analysis was carried out using the protocol reported in section 4.2.10.5.

5.2.8.6. Biochemical analysis

The biochemical analysis was carried out using the protocol reported in section 4.2.10.6.

5.2.8.7. Statistical analyses

All values are expressed as the mean ± SEM. One-way ANOVA followed by Newman-Keuls multiple comparison post-hoc test was performed.

5.3. Results and discussion

5.3.1. Chemistry

The synthesis was initiated by dissolving *phenylglycine* (**1**) in an aqueous *sodium carbonate* solution, wherein the carboxylic acid reacted with sodium carbonate to form the water-soluble sodium salt of *phenylglycine*. *Benzene sulfonyl chloride* (**2**) was dissolved in acetone separately. Acetone was also added to the reaction mixture that provided miscibility to *benzene sulfonyl chloride* (**2**) solution and facilitated reaction in a monophasic medium. The reaction followed a similar mechanism as reported in section

4.3.2. Finally, the acidification of the reaction mixture led to precipitation of, *S-(+)-2-phenyl-2-(phenylsulfonamido) acetic acid* (**3**), due to the common ion effect. The white solid residue was washed with cold water to remove the trace amount of the *benzene sulfonic acid*. The synthesis of various amide derivatives (**26 – 44**) by reaction with substituted anilines (**4 – 25**) in the presence of *triethylamine* and *thionyl chloride* is depicted in scheme **(Scheme 1)** (**Figure 5.2**).

Step-1: Synthesis of sulfonamide derivative of α-phenylglycine

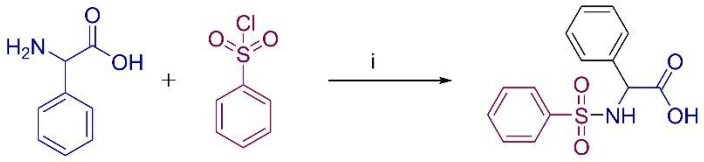

1 2 3

Step-2: Synthesis of derivatives of (*S)-(+)-N,2-diphenyl-2-(phenylsulfonamido) acetamide*

Scheme 1

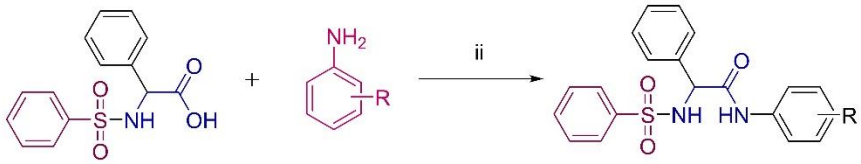

3 4-22 26-44

Comp code	4, 26	5, 27	6, 28	7, 29	8, 30	9, 31	10, 32	11, 33	12, 34
R	H	2-F	3-F	4-F	2-Cl	3-Cl	4-Cl	2-Br	3-Br

Comp code	13, 35	14, 36	15, 37	16, 38	17, 39	18, 40	19, 41	20, 42	21, 43	22, 44
R	4-Br	2-OCH_3	3-OCH_3	4-OCH_3	3-NO_2	4-NO_2	2-CH_3	3-CH_3	4-CH_3	2-C_2H_5

Scheme 2

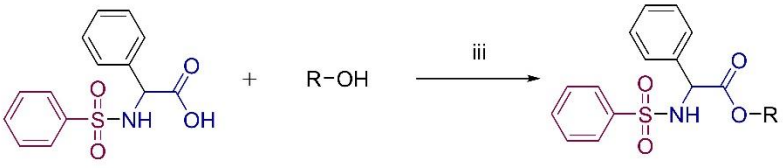

3 23-25 45-47

Comp code	23, 45	24, 46	25, 47
R	CH_3	C_2H_5	C_4H_9

(i) Na_2CO_3, Water:Acetone mixture, rt (ii) TEA, $SOCl_2$, DCM, rt (iii) $SOCl_2$, rt

Figure 5.2 Reaction scheme for synthesis of (S)*-(+)-N,2-diphenyl-2-(phenylsulfonamido) acetamide* derivatives.

The yield of the compounds **26 – 44** was found to be 47.25 – 94.90 %. The melting point of compounds showed variation with the *ortho* derivatives displayed lower melting points than the corresponding *meta*- and *para*-derivatives. The highest melting points (183 – 187 and 185 – 189 ºC) were recorded for *meta*- and *para*- *nitro* derivatives, respectively. The R_f value of *chloro, bromo, methyl* and *ethyl* derivative were found to be higher than other compounds of **Scheme 1**. The *nitro* and *methoxy* derivatives were found to be more polar with lower R_f values in the series. The synthesis of esters of *S-(+)-2-phenyl-2-(phenylsulfonamido) acetic acid* (**3**) is depicted in the scheme (**Scheme 2**). The esters were synthesised in the presence of *thionyl chloride* and corresponding alcohols in the absence of *triethylamine*. The esters displayed an excellent yield in a range of 85.86 – 95.59 %. The R_f values of the compounds **45 – 47** were found to be highest among all the compounds. The melting points also followed a trend in increasing the order of their molecular weights. The ^{1}H NMR displayed that the proton of the *amide* bond produced a downfield signal and was the most deshielded proton. It was observed that the *ortho*-substitutions of the *phenyl* ring linked to *amide* nitrogen displayed more shielding of the NH proton than *para*-position. However, the substitutions at the *meta*-position displayed the highest deshielding effect on amide proton. The *nitro* group displayed the highest deshielding of the *amide* proton due to the negative mesomeric or electro withdrawing effect. On the other hand, the *ortho-ethyl* group present on the *phenyl* ring displayed a strong positive mesomeric or electron-donating effect rendering this signal upfilled among all the compounds. This signal was absent in all the ester derivatives and thus established that the signal in this range was due to the presence of an *amide* proton. The second most prominent signal was of proton of the *sulfonamide* group. The signal was present in the range of 8.92 – 8.72 ppm. The third prominent signal was of *methine* proton that displayed a signal in the range of 5.5 – 4.75 ppm. It was observed that protons of sulfonamide NH and *methine* displayed a strong long-range coupling, hence causing the

splitting of proton signals into doublets. The aromatic protons remained at the expected position of 6.5 – 8.5 ppm. The ^{13}C NMR displayed a signal of *carbonyl* carbon around 167 ppm which was slightly higher for the esters. The *methine* carbon displayed signal around 60 ppm. This deshielding was observed due to the presence of *amine, phenyl* and *carbonyl* groups adjacent to the methine. The aromatic carbons displayed peaks in the expected region of the spectra. The infra-red spectra of the synthesised compounds displayed characteristic peaks of all the functional groups. The mass spectra of *chloro* and *bromo* derivatives displayed M^+ and M^{+2} peaks in a ratio of 3:1 and 1:1, respectively.

5.3.2. *In vitro* ChE inhibitory activity

Compound **26** displayed BChE inhibition of 52.66 ± 4.53 % at a concentration of 50 µM. The substitution of *fluoro* group at *ortho* and *para* position (**27**, 69.17 ± 1.33 % and **29**, 71.53 ± 7.32 %, respectively) resulted in higher inhibition of BChE than compound **26**. However, the *meta-fluoro* derivative displayed BChE inhibition of only 1.23 ± 0.84 %. The substitution of *fluoro* with the *chloro* group at *ortho*-position resulted in increased BChE inhibition of compound **30** (86.04 ± 0.35 %). The *meta* (**31**) and *para*-substitution (**32**) showed low inhibitions of 10.79 ± 0.68 and 11.99 ± 0.55 %, respectively. The *bromo* substitution also displayed a similar trend and *ortho-bromo* substituted compound **33** displayed 83.77 ± 0.74 % BChE inhibition. On the other hand, *meta-* and *para-bromo* derivatives, i.e., compounds **34** and **35**, displayed low inhibition of 10.63 ± 0.15 and 11.54 ± 1.85 %, respectively. In contrast, the *methoxy* group, showing a strong mesomeric effect than the halogen derivatives, displayed an opposite trend. *The meta-methoxy* substituted compound **37** produced higher inhibition of about 41.77 ± 0.62 %, while the *ortho-* and *para*-substituted compounds **36** and **38** displayed inhibition of 26.94 ± 1.02 and 20.31 ± 0.7 %, respectively. Further, the strong electron-withdrawing effect of the *nitro* group also adversely affected the inhibitory activity. The *meta-* and *para-nitro* derivatives (**39** and **40**) displayed inhibition of 16.13 ± 0.73 and 19.28 ± 0.4 %, respectively. The electron

releasing effect of the *methyl* group at *ortho*- and *para*-positions rendered compounds **41** and **43** inactive. The *meta-methyl* substitution (**42**) resulted in BChE inhibition of 15.77 ± 2.72 %. In contrast, the *ortho-ethyl* (**44**) substitution produced a significantly higher inhibition of BChE to 69.76 ± 0.37 %.

Table 5.1 Inhibition of BChE and AChE by compounds (**26 – 47**) at a concentration of 50 µM.

Compound code	**% Inhibition**	
	BChE	**AChE**
26	52.66 ± 4.53	2.29 ± 1.19
27	69.17 ± 1.33	8.15 ± 0.48
28	1.23 ± 0.84	5.82 ± 0.78
29	71.53 ± 7.32	9.41 ± 1.39
30	86.04 ± 0.35	1.62 ± 1.49
31	10.79 ± 0.68	na
32	11.99 ± 0.55	1.32 ± 2.65
33	83.37 ± 0.74	0.38 ± 1.92
34	10.63 ± 0.15	na
35	11.54 ± 1.85	na
36	26.94 ± 1.02	10.72 ± 1.51
37	41.77 ± 0.62	14.03 ± 0.85
38	20.31 ± 0.7	2.74 ± 0.87
39	16.13 ± 0.73	9.02 ± 1.36
40	19.28 ± 0.4	7.89 ± 1.41
41	na	3.91 ± 0.47
42	15.77 ± 2.72	8.56 ± 0.11
43	na	3.02 ± 1.02
44	69.76 ± 0.37	25.85 ± 7.1
45	15.63 ± 1.31	4.46 ± 0.75
46	29.09 ± 1.62	15.7 ± 5.92
47	32.42 ± 1.15	7.27 ± 3.72

Data are expressed as Mean ± SEM. na – not active

Table 5.2 IC_{50} of selected compounds against BChE.

Compound code	**IC_{50} (µM)**
27	16.915 ± 1.6
29	12.204 ± 1.3
30	7.331 ± 0.946
33	10.964 ± 0.936
44	20.892 ± 1.31

Data are expressed as Mean ± SEM.

The results indicated that the *ortho*-position was critical for BChE inhibition. All the *ortho*-substituted compounds, except *ortho-methoxy* and *methyl* derivatives, displayed

good inhibition. In contrast, only *para-fluoro* derivative displayed higher BChE inhibition and *meta-methoxy* derivatives displayed a fair inhibition. The esters displayed increasing inhibition in order of their molecular weight with *methyl* (**45**), *ethyl* (**46**) and *butyl* (**47**) esters of compound **3** displaying 15.63 ± 1.31, 29.09 ± 1.62 and 32.42 ± 1.15 % inhibitions, respectively (**Table 5.1**).

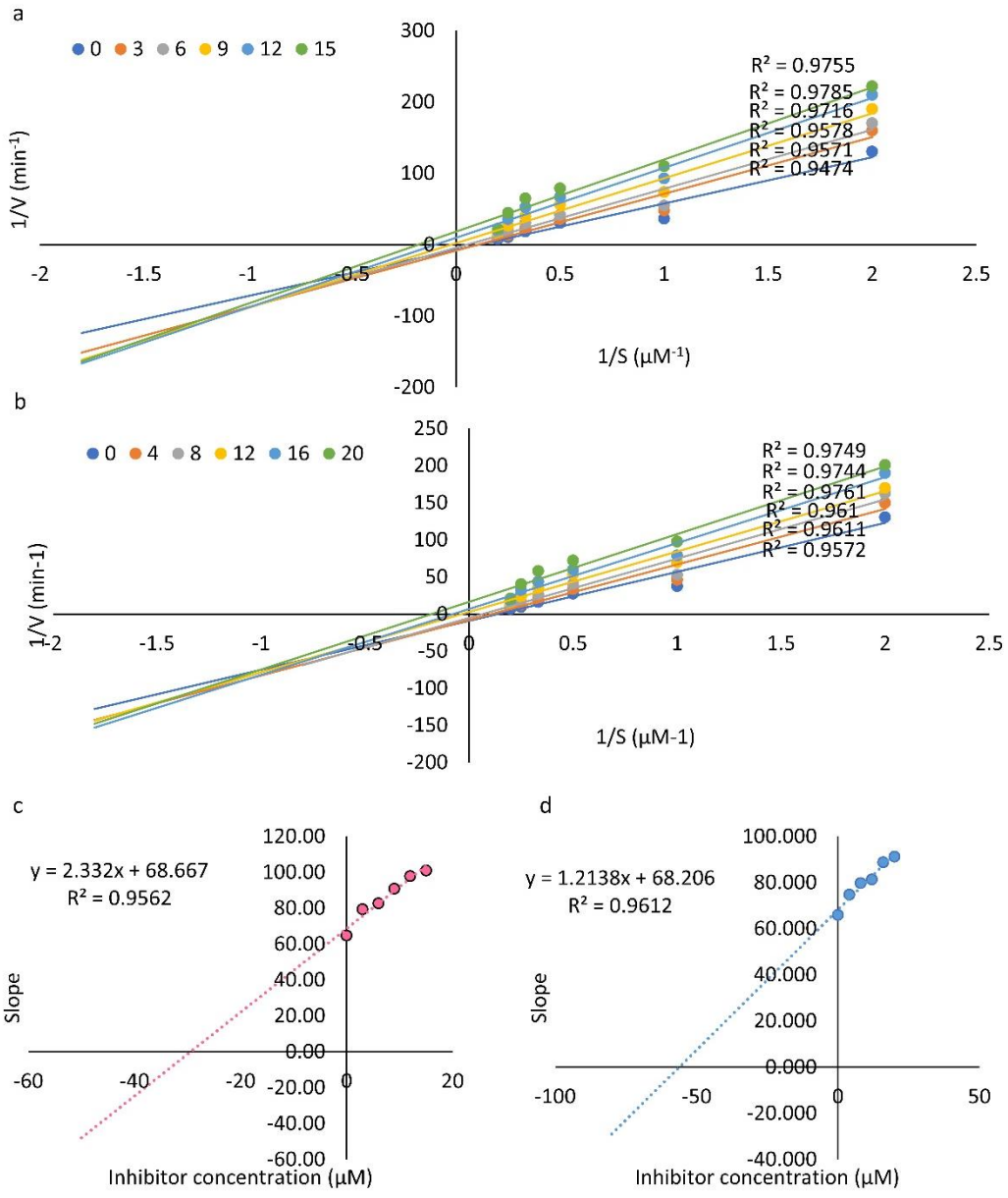

Figure 5.3 Lineweaver Burk double reciprocal plot of compounds (a) **30** and (b) **33**. Dixon plot of compound (a) **30** and (b) **33** for Ki calculation.

The AChE inhibition was also determined at a concentration of 50 µM. Interestingly, compounds **36** (*ortho-*OCH_3, 10.72 ± 1.51 %), **37** (*meta-*OCH_3, 14.03 ± 0.85 %) and **44**

(*ortho-ethyl*, 25.85 ± 7.1) displayed AChE inhibition above 10 % among all the compounds of the **scheme 1**. The *ethyl* ester (46) displayed 15.7 ± 5.92 % of AChE inhibition among the ester derivatives. Further, IC_{50} values were determined for the five most potent compounds that displayed inhibition of above 60 % at a concentration of 50 µM. Compound **30 (***ortho- chloro* derivative) displayed the lowest IC_{50} value of 7.331 ± 0.946 µM followed by the *ortho-bromo* derivative **33** with IC_{50} of 10.964 ± 0.905 µM. The IC_{50} values are presented in table **(Table 5.2)**. The double reciprocal Lineweaver Burk plot indicated that compounds **30** and **33** inhibited BChE in a non-competitive fashion. In the third quadrant of the plot, the intersecting lines converged, showing that the inhibitors had a higher affinity for the enzyme-substrate complex ($\alpha < 1$) than for free enzyme. Dixon plots were also used to calculate the inhibition constant (Ki). The compounds **30** and **33** had the inhibition constant of 29.44 and 56.23 µM, respectively (**Figure 5.3**).

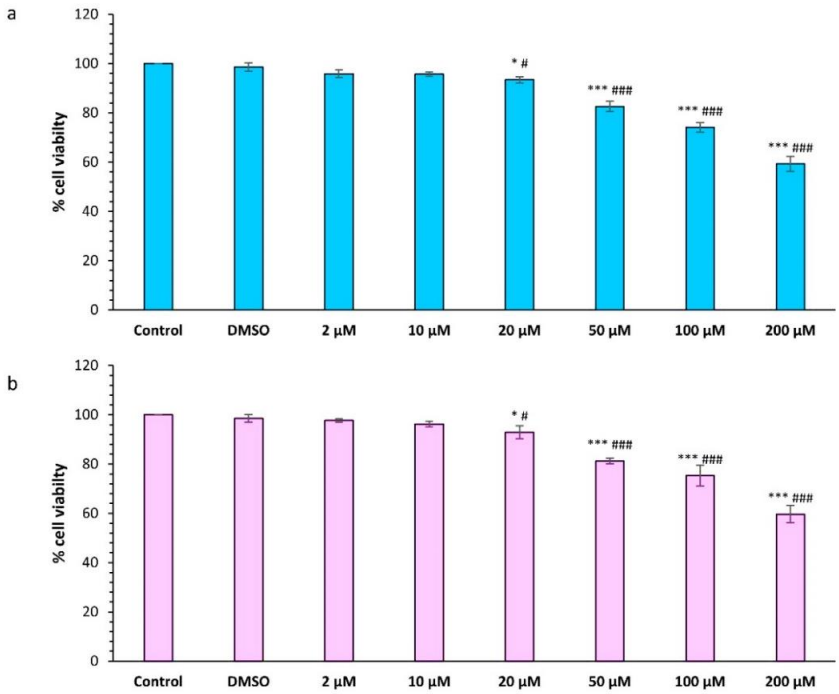

Figure 5.4 Cell viability assay of compounds (a) **30** and (b) **33** on SH-SY5Y cells. PBS was taken as control. Data are expressed as Mean ± SD. One-way ANOVA was applied followed by Newman-Keuls multiple comparison test to compare all column pairs ($^{*}p < 0.05$ compared to control; $^{***}p < 0.001$ compared to control; $^{\#}p < 0.05$ compared to DMSO; $^{\#\#\#}p < 0.001$ compared to DMSO).

5.3.3. Cell viability (MTT Assay)

The cell viability, at a concentration of 200 µM, was found to be 59.28 ± 3.08 and 59.69 ± 3.49 % for compounds **30** and **33,** respectively. There was a significant reduction in the cell viability in a dose-dependent manner from 20 µM concentration. The figure **(Figure 5.4)** presents the cell viability of the compounds at different concentrations.

5.3.4. *In vitro* blood-brain barrier permeation assay

Compounds **30** and **33,** selected on the basis of cell viability study, were evaluated for BBB permeability. The permeability (Pe) values of the compounds are listed in the table **(Table 5.3)**. Both the halogen derivatives were found to be permeable.

Table 5.3 Permeability data for selected compounds from the PAMPA-BBB assay.

Compound code	Pe (10^{-6} cm s^{-1})
30	6.459 ± 0.67
33	6.183 ± 0.745

All data are expressed as Mean ± SD for the experiment performed in triplicates.
Compounds with Pe > 4.324×10^{-6} cm s^{-1} could cross the BBB (CNS+), Pe < 1.846×10^{-6} cm s^{-1} could not cross the BBB (CNS−) and 1.846×10^{-6} cm s^{-1} < Pe < 4.324×10^{-6} cm s^{-1} showed uncertain BBB permeation (CNS ±).

5.3.5. *In silico* ADMET and molecular properties analyses

In the current study, no molecule was found to violate RO5 and PAINS filter. The designed molecules have logP value above 3. The halogen derivatives (**27** – **35**) showed an increase in the logP value with an increase in atomic mass. The *methoxy* and *nitro* derivatives (**36** – **40**) have a lower logP value than the halogen derivatives. The *methyl* and *ethyl* substituents showed an increase in the logP values. On the other hand, the ester derivatives showed logP lower than other compounds with a positive correlation between LogP value and size of alkyl chain substitution in ester. The CNS permeability prediction indicated that the *bromo* derivative compounds **33** – **35** were most permeable and others were moderately CNS permeable. All of the compounds in the series were predicted to be substrates for CYP3A4 rather than CYP2D6 and were also non-inhibitors of the hERG 1 channel, which controlled the cardiac cycle's plateau phase (**Table 5.4**).

Table 5.4 Molecular and selected ADME properties of synthesised compounds.

Compound code	LOGP	Intestinal absorption (human)	CNS permeability	CYP2D6 substrate	CYP3A4 substrate	CYP2D6 inhibitor	CYP3A4 inhibitor	hERG I inhibitor
26	3.344	92.605	-2.131	No	Yes	No	Yes	No
27	3.484	91.771	-2.168	No	Yes	No	Yes	No
28	3.484	92.723	-2.186	No	Yes	No	Yes	No
29	3.484	92.011	-2.17	No	Yes	No	Yes	No
30	3.998	90.944	-2.011	No	Yes	No	Yes	No
31	3.998	91.815	-2.02	No	Yes	No	Yes	No
32	3.998	91.13	-2.013	No	Yes	No	Yes	No
33	4.107	90.877	-1.989	No	Yes	No	Yes	No
34	4.107	91.748	-1.998	No	Yes	No	Yes	No
35	4.107	91.063	-1.991	No	Yes	No	Yes	No
36	3.353	92.526	-2.288	No	Yes	No	Yes	No
37	3.353	94.123	-2.31	No	Yes	No	Yes	No
38	3.353	93.504	-2.3	No	Yes	No	Yes	No
39	3.253	85.816	-2.345	No	Yes	No	No	No
40	3.253	85.798	-2.342	No	Yes	No	No	No
41	3.653	92.403	-2.052	No	Yes	No	Yes	No
42	3.653	93.274	-2.061	No	Yes	No	Yes	No
43	3.653	92.588	-2.054	No	Yes	No	Yes	No
44	3.907	91.446	-2.079	Yes	Yes	No	Yes	No
45	1.879	94.381	-2.55	No	Yes	No	No	No
46	2.269	93.934	-2.549	No	Yes	No	No	No
47	3.049	94.172	-2.544	No	Yes	No	No	No
Donepezil	4.361	92.731	-1.437	Yes	Yes	Yes	Yes	No

5.3.6. Molecular docking

Molecular docking of the active compounds **26**, **27**, **29**, **30**, **33**, **37** and **44** provided some crucial information which is presented in figures (**Figures 5.5** and **5.6**). The binding of prototype compound **26** indicated that the *phenyl* ring attached to the *sulfonyl* group formed π-π interaction with Trp82 and π-alkyl interaction with the side chain of Ala328. The *sulfonyl* group formed π-sulfur interaction with His438. The *carbonyl* group of the *amide* bond formed a hydrogen bond with Gly117. The Trp231 and Phe329 formed π-π interactions and Leu286 formed π-alkyl interactions with the *phenyl* ring attached to the *amide* bond. Further, there was no significant contribution by *phenyl* ring originated from

the *phenylglycine* of the scaffold. This was in contrast to the parent compound **II (Figure 5.1)** in which the central *phenyl* ring of the *para-amino benzoic acid* contributed to the ligand binding.

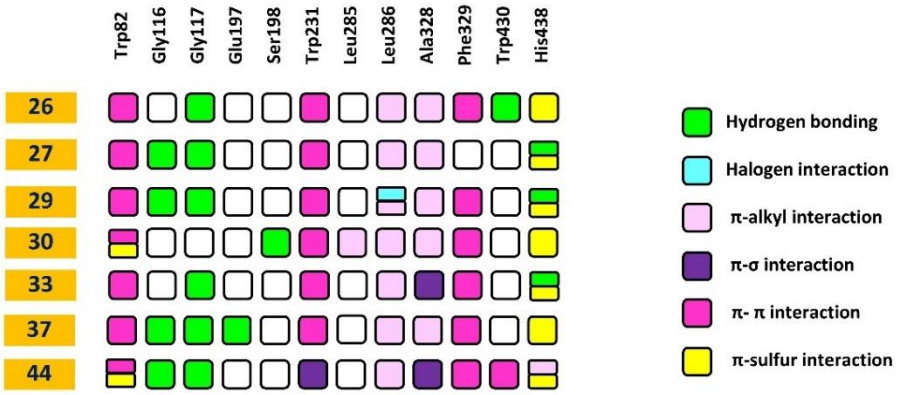

Figure 5.5 Interaction profile of ligands with BChE.

Compounds **27**, **30** and **33,** the *ortho halogen*-substituted derivatives of compound **26,** displayed π-π and π-alkyl interactions with Trp82 and Ala328, respectively, with additional π-sulfur interaction with Trp82. His438 displayed a π-sulfur interaction with *sulfonyl* group in all the compounds with an additional hydrogen bond in the case of compound **27**. The *phenyl* ring connected through the *amide* bond showed interactions with Trp231 and Leu286. The *bromo* derivative (**33**) showed an additional π-π interaction with Phe329. Compound **30** displayed a different orientation compared to compounds **26**, **27** and **33**. This led to a change in the interactions of *carbonyl* groups of Gly116, Gly117 with compound **27**, Gly117 with compound **33** and Ser198 with compound **30**. However, the most interesting observation with compound **30** was the interaction of the central *phenyl* ring with Leu285, Ala328 and Phe329. The additional interaction was reflected in inhibition data and IC_{50} value, rendering compound **30** to be most potent among all. In case of *bromo* derivative (**33**), the interaction with Ser198 through hydrogen bonding improved the binding as compared to compound **27**. The *para-fluoro* derivative (**29**) displayed similar interactions to compound **27**. Further, it showed two additional

interactions, i.e., halogen and π-alkyl interactions with Leu286 and π-π interaction with Phe239, which contributed to its higher potency than compound **27**.

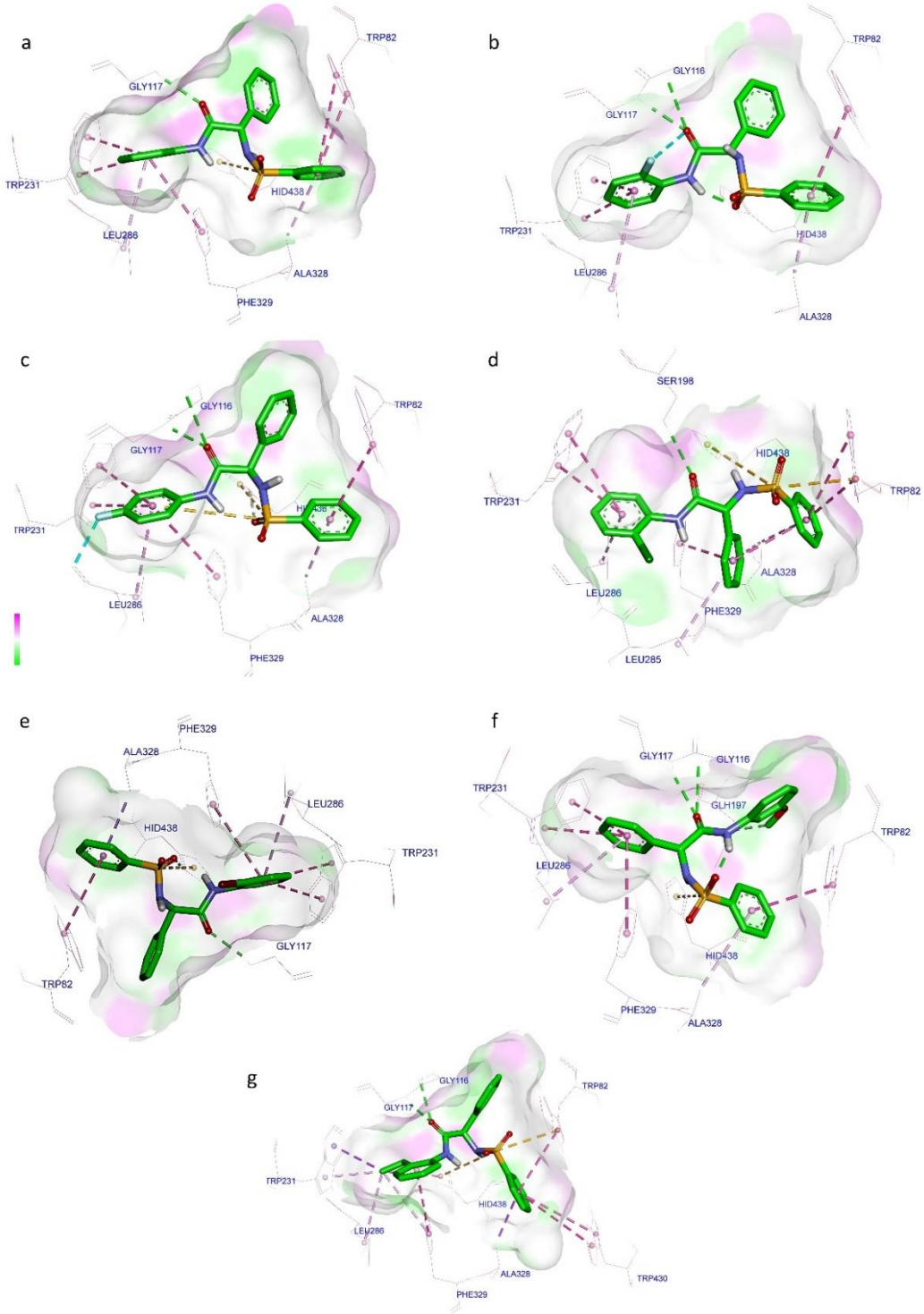

Figure 5.6 3D interaction of compounds (a) **26**, (b) **27**, (c) **29**, (d) **30**, (e) **33**, (f) **37** and (g) **44** with BChE.

Compound **44** showed similar interactions to that of **27**, the modest change in its interaction pattern was reflected in the inhibition data too. The *ortho ethyl* group

interacted with Trp231, Leu286 and His438, while the *phenyl* ring showed interaction with Phe239. Compound **37** also displayed similar interactions to that of **30,** but the *phenyl* ring connected through the *amide* bond displayed only a hydrogen bond with Glu197. This resulted in limited interaction of *phenyl*, as the solvent exposure caused a decrease in potency. The binding energies of the compounds are reported in the table **(Table 5.5)**.

Table 5.5 Binding energies of the selected compounds.

Compound code	Binding energies (Kcal/mol)
26	-8.45
27	-8.64
29	-8.36
30	-8.6
33	-8.72
37	-8.01
44	-8.34

5.3.7. Molecular dynamics

In the present study, MD simulations were carried out for the most active ligands **30**, **33** and donepezil, complexed with the BChE. The energy minimisation led to the change in total potential energy from -194630, -194670, -194700 and -194450 to -298650, -298950, -298840 and -298490 Kcal/mol, for BChE, BChE complexed with compounds **30**, **33** and donepezil, respectively. All the complexes attained the desired temperature of 310.15 K within 5 – 6 ps and the temperature was maintained for the rest of the time during heating. The mean temperatures were 310.08 ± 1.16, 310.31 ± 1.04, 310.23 ± 1.11 and 310.03 ± 1.07 K, for BChE, BChE complexed with compounds **30**, **33** and donepezil, respectively. During density equilibration, the unit density of the complexes was attained at 50^{th} ps of the run. The mean densities were 1.011 ± 0.003. 1.011 ± 0.002, 1.01 ± 0.003 and 1.011 ± 0.003 g/cm^3, for BChE, BChE complexed with compounds **30**, **33** and donepezil, respectively. Finally, a one ns MD stimulation was carried out under constant NPT conditions to evaluate the stability of the prepared system before MD. The mean RMSD was found to 1.005 ± 0.138, 0.943 ± 0.078, 0.920 ± 0.074 and 1.076 ± 0.137 Å, for BChE,

BChE complexed with compounds **30**, **33** and donepezil, respectively (**Figures S6 – S9 in SI**).

The mean RMSD(s) values were 1.283 ± 0.153, 1.345 ± 0.188, 1.202 ± 0.119 and 1.335 ± 0.122 Å, for BChE, BChE complexed with compounds **30**, **33** and donepezil, respectively. The RMSD for the BChE complex with compound **33** was slightly lower than the other two ligands. However, there was no significant difference among the complexes, thus indicating a stable RMSD. It was found that mean RMSD(s) were 1.103 ± 0.364, 0.429 ± 0.124 and 1.785 ± 0.276 Å, for compounds **30**, **33** and donepezil, respectively. The results indicated that the designed BChE inhibitors were more stable in the cavity of the protein than donepezil. However, all three ligands showed acceptable RMSD values (**Figure 5.7**). Overall, the RMSF of complexes did not show much deviation. However, the residue analysis revealed that compound **30** stabilised Asp70, Trp82, Leu286, Leu288 and Glu285. In the case of compound **33**, stability was observed for all crucial residues viz. Asp70, Trp82, Gly116, Gly117, Ser198, Ala199, Leu286, Leu288, Tyr332 and His438. Donepezil stabilised Trp82, Ser198, Ala199, Glu235 and Tyr332 as compared to the uninhibited enzyme. RMSF of compound **30** indicated that the *phenyl* rings attached to *sulfonyl* and *amide* groups had higher atomic fluctuations. On the other hand, all the atoms showed similar fluctuations in the case of compound **33** and donepezil. Overall, compound **33** showed much lower RMSF than others. The mean SASA was 21113.978 ± 374.686, 20833.058 ± 401.907, 20877.935 ± 349.762 and 21309.959 ± 404.557 $Å^2$, for BChE, BChE complexed with compounds **30**, **33** and donepezil, respectively. In the case of compounds **30** and **33**, SASA was decreased, as compared to the uninhibited enzymes, and thus indicating the ligand binding to solvent-exposed amino acid residues (**Figure 5.8**). On other hand, the binding of donepezil

marginally increased SASA. The mean SASA was found to be 132.213 ± 33.097, 60.637 ± 13.91 and 109.602 ± 21.665 $Å^2$, for compounds **30**, **33** and donepezil, respectively.

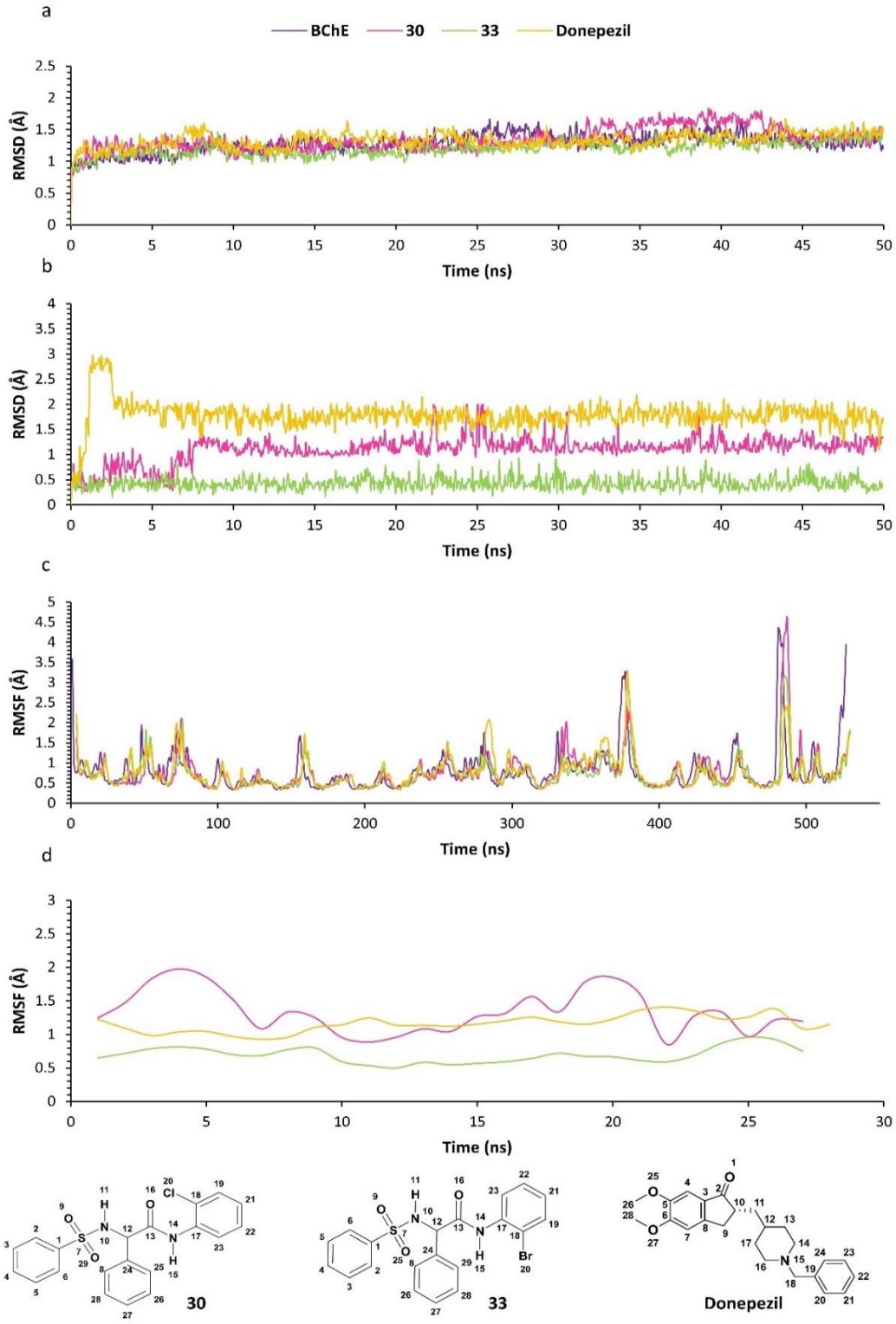

Figure 5.7 RMSD and RMSF analysis of BChE, BChE complexed with compounds **30**, **33** and donepezil: (a) RMSD of protein backbone. (b) RMSD of heavy atoms of ligands. (c) RMSF of protein backbone. (d) RMSF of heavy atoms of ligands.

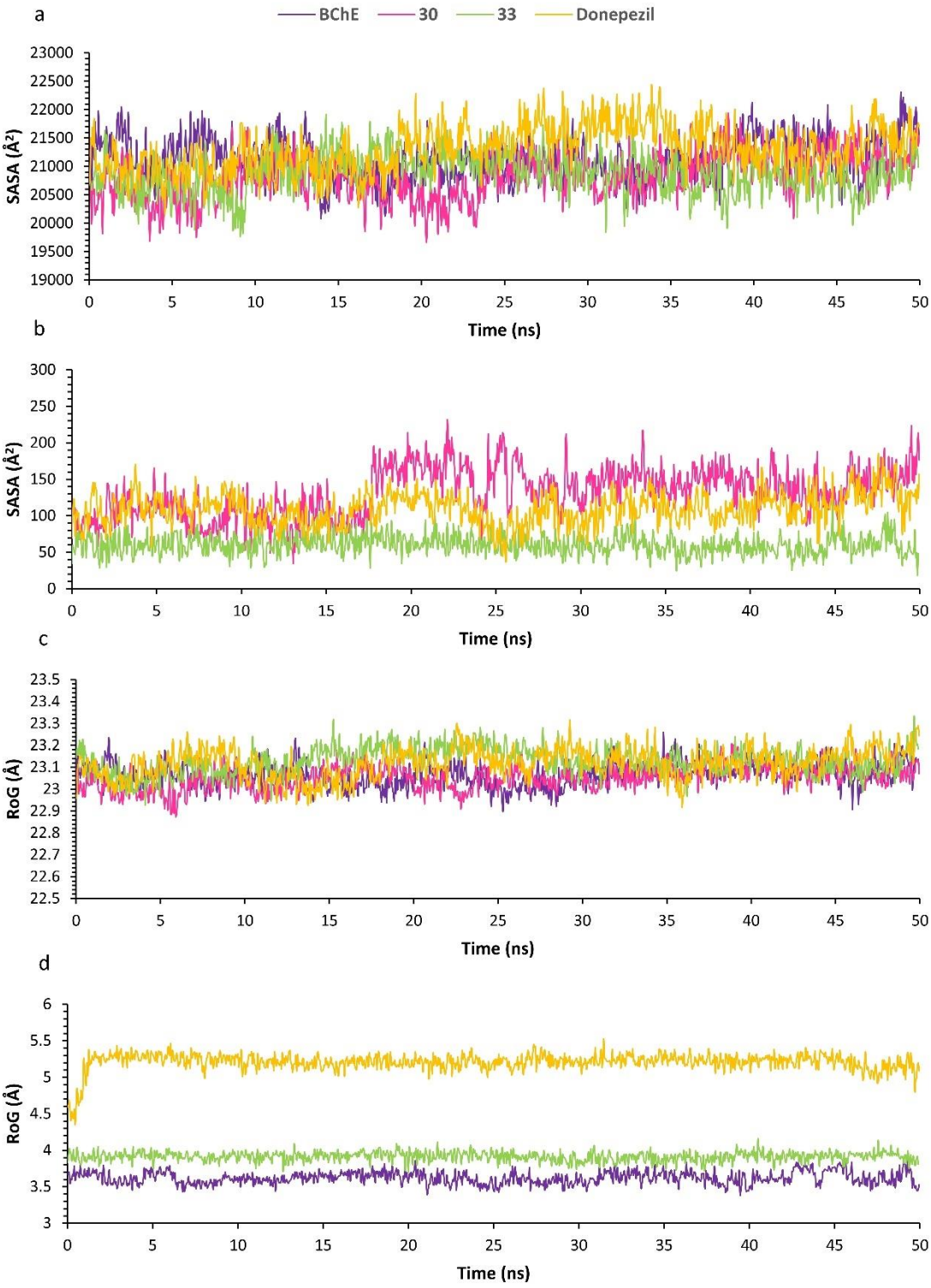

Figure 5.8 SASA and RoG analysis of BChE, BChE complexed with compounds **30**, **33** and donepezil: (a) SASA of protein-ligand complexes. (b) SASA of ligands. (c) RoG of protein-ligand complexes. (b) RoG of ligands.

The mean RoG were 23.066 ± 0.056, 23.052 ± 0.055, 23.129 ± 0.061 and 23.118 ± 0.069

Å, for BChE, BChE complexed with compounds **30**, **33** and donepezil, respectively.

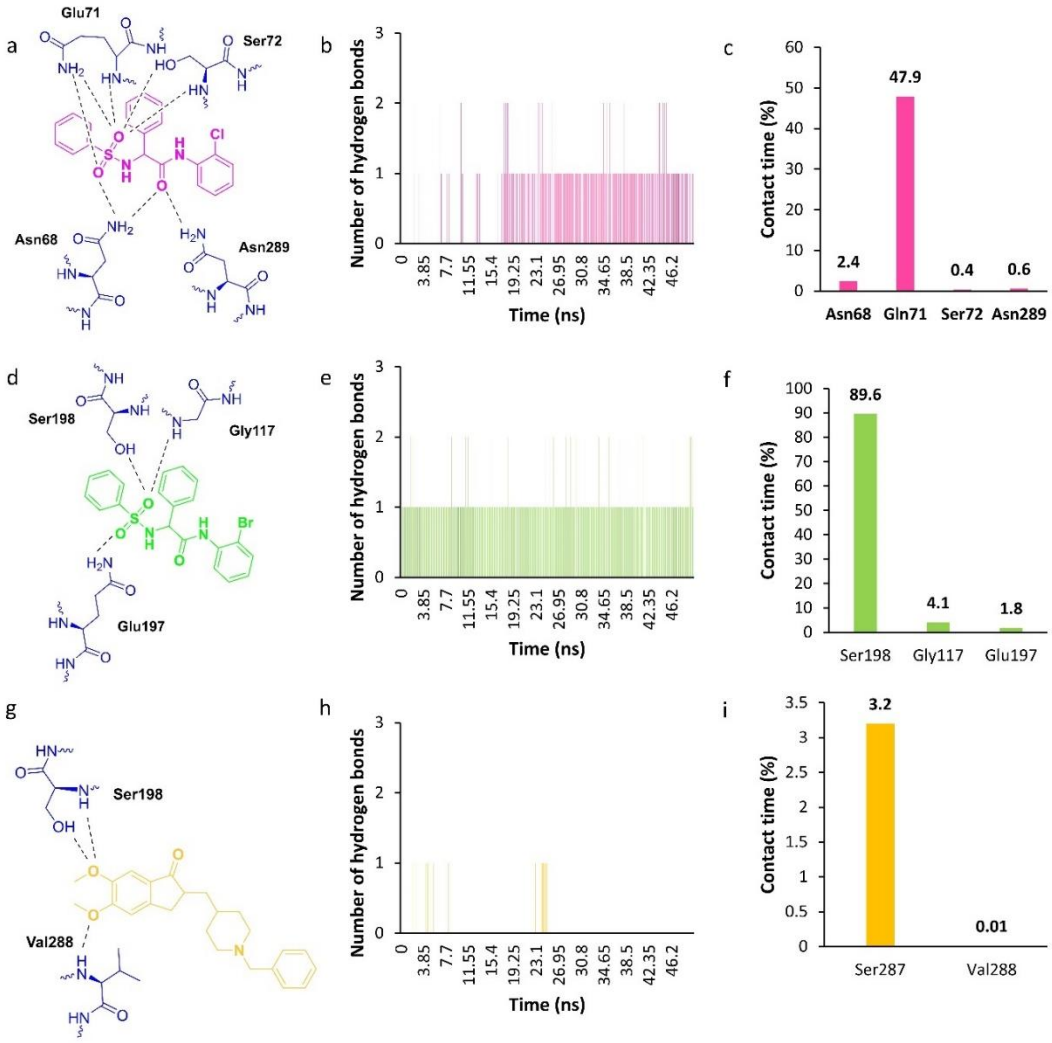

Figure 5.9 (a, d, g) Hydrogen bond interaction of the compounds **30**, **33** and donepezil with residues, respectively. (b, e, h) Number of hydrogen bonds formed by compounds **30**, **33** and donepezil with enzyme over the period of 50 ns, respectively. (c, f, i) Contact time of crucial residues with compounds **30**, **33** and donepezil, respectively.

There were no significant changes in RoG(s) on binding with the ligands. The mean RoG of compounds **30**, **33** and donepezil was 3.62 ± 0.086, 3.913 ± 0.066 and 5.207 ± 0.121 Å, respectively. Thus, the designed compounds had a smaller size as compared to donepezil. The hydrogen bond analysis indicated that compound **30** produced hydrogen bonding with Asn68, Glu71, Ser72 and Asn289, while compound **33** with Gly117, Glu197 and Ser198. Donepezil formed hydrogen bonds with Ser287 and Val288. The *sulfonamide* group was responsible for the prominent hydrogen bonding of the synthesised compounds (**Figure 5.9**).

5.3.8. *In vivo* evaluation of compounds

5.3.8.1. Y-maze

5.3.8.1.1. Effects of scopolamine and various treatments on spontaneous alteration

The treatment with SCO displayed a significant decrease in the spontaneous alteration in the rat as compared to control ($P < 0.001$, group: II vs I). However, treatment with donepezil resulted in significant improvement in % spontaneous alteration by reducing the effect of SCO treatment ($P < 0.01$, group: III vs. II). In case of compound **30**, there was a significant increase in the spontaneous alteration, except at the dose of 5 mg/Kg. The spontaneous alterations at doses of 10 and 20 mg/Kg were significantly higher than that of SCO ($P < 0.01$, group: V vs. II and VI vs. II) whereas, a dose of 5 mg/Kg of the compound **30** produced less alteration ($P < 0.05$, group: V vs. IV and VI vs. IV). The compound **33** also displayed a similar trend. It was observed that the doses of 10 and 20 mg/Kg produced significantly higher spontaneous alterations than SCO treatment ($P < 0.01$, group: VIII vs. II and IX vs. II). The improvement in alteration was less at the dose of 5 mg/Kg ($P < 0.05$, group: VIII vs. VII and $P < 0.01$, group: IX vs. VII) (**Figure 5.10 (a)**).

5.3.8.1.2. Effect of scopolamine and various treatments on novel arm entries

SCO treatment also displayed a significant reduction in the novel arm entries as compared to the control group ($P < 0.001$, group: II vs. I). Donepezil also produced significant improvement in novel arm entries in comparison to SCO treatment ($P < 0.001$, group: III vs. II). The treatment with compound **30,** at doses of 10 and 20 mg/Kg, resulted in significant improvement in the novel arm entries as compared with SCO ($P < 0.001$, group: V vs. II and V vs. II), but the effect was reduced at a dose of 5 mg/Kg ($P < 0.05$, group: V vs. IV and VI vs. IV). Similarly, compound **33** also displayed significant improvement in novel arm entries for the doses of 10 and 20 mg/Kg as compared to SCO ($P < 0.001$, group: VIII vs. II and IX vs. II) (**Figure 5.10 (b)**).

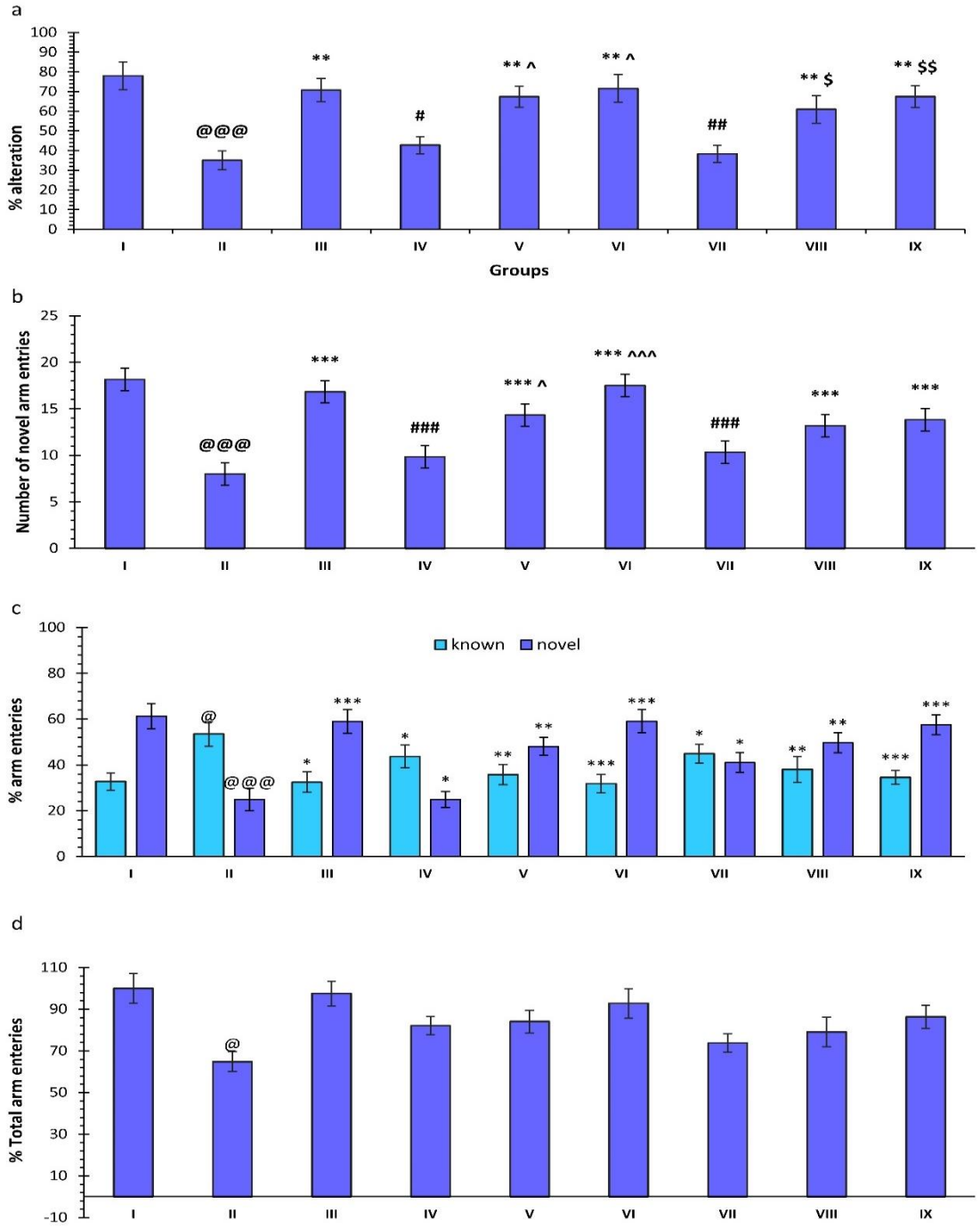

Figure 5.10 Effect of compounds **30, 33** and donepezil on (a) scopolamine-induced impairment of % spontaneous alteration, (b) novel arm entries, (c) % arm entries and (d) % total arm entries.

Data are expressed in Mean ± SEM (N =6, $^{@@@}$ P < 0.001 compared to control, * P < 0.05 compared to SCO, ** P < 0.01 compared to SCO, *** P < 0.001 compared to SCO, $^{\#}$ P < 0.05 compared to donepezil , $^{\#\#}$ P < 0.01 compared to donepezil , $^{\#\#\#}$ P < 0.001 compared to donepezil , $^{\wedge}$ P < 0.05 compared to compound **30**(5 mg/Kg), $^{\wedge\wedge}$ P < 0.01 compared to compound **30**(5 mg/Kg), $^{\wedge\wedge\wedge}$ P < 0.001 compared to compound **30**(5 mg/Kg), $^{\$}$ P < 0.05 compared to compound **33**(5 mg/Kg), $^{\$\$}$ P < 0.01 compared to compound **33**(5 mg/Kg) , $^{\$\$\$}$ P < 0.001 compared to compound **33**(5 mg/Kg)).

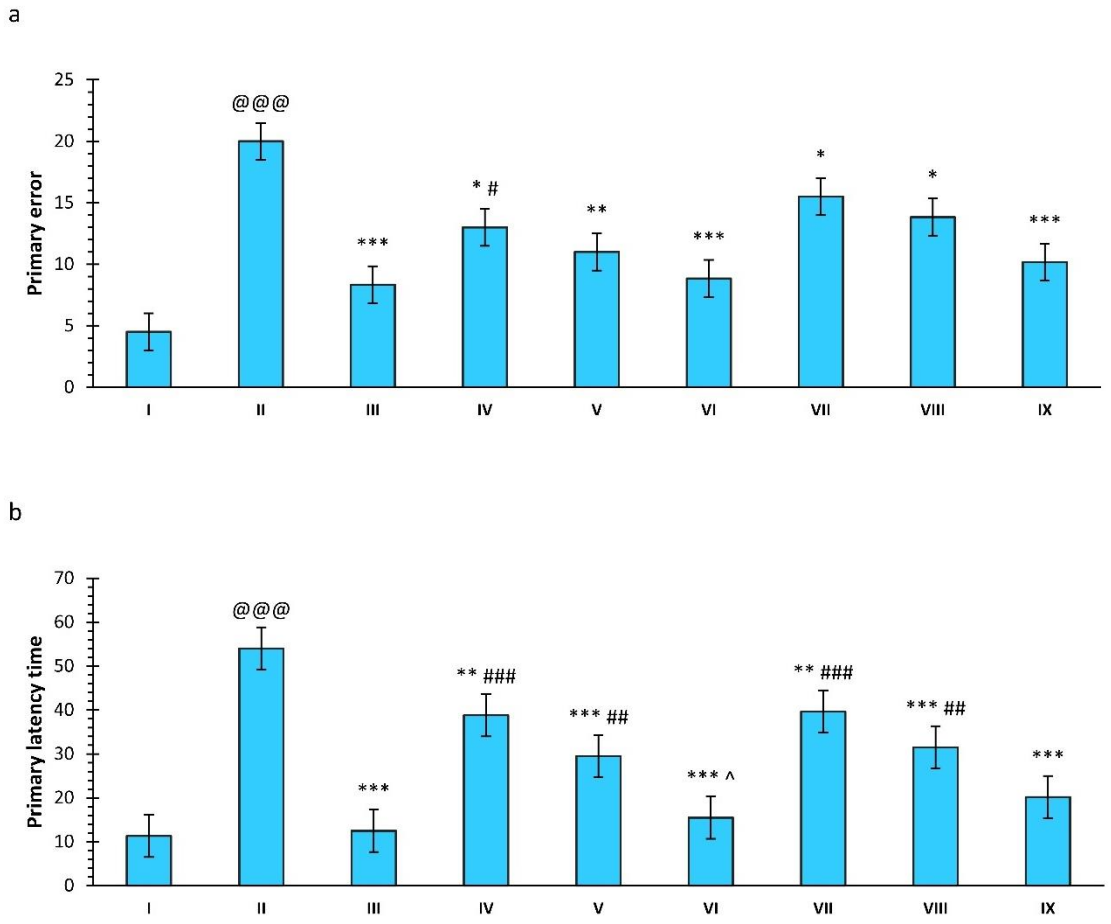

Figure 5.11 Effect of compounds **30, 33** and donepezil on (a) primary error, (b) primary latency time.

Data are expressed in Mean ± SEM (N =6, $^{@@@}$ P < 0.001 compared to control, * P < 0.05 compared to SCO, ** P < 0.01 compared to SCO, *** P < 0.001 compared to SCO, $^{\#}$ P < 0.05 compared to donepezil , $^{\#\#}$ P < 0.01 compared to donepezil , $^{\#\#\#}$ P < 0.001 compared to donepezil , $^{\wedge}$ P < 0.05 compared to compound **30**(5 mg/Kg), $^{\wedge\wedge}$ P < 0.01 compared to compound **30**(5 mg/Kg), $^{\wedge\wedge\wedge}$ P < 0.001 compared to compound **30**(5 mg/Kg), $^{\$}$ P < 0.05 compared to compound **33**(5 mg/Kg), $^{\$\$}$ P < 0.01 compared to compound **33**(5 mg/Kg) , $^{\$\$\$}$ P < 0.001 compared to compound **33**(5 mg/Kg))

5.3.8.1.3. Effect of scopolamine and various treatments on percentage novel and known arm entries

SCO treatment group showed a significant increase in the % known arm entries in comparison to control (P < 0.05, group: II vs. I). In case of compounds **30** and **33**, an increase was observed at a dose of 5 mg/Kg. On the other hand, there was no significant change in known arm entries in any of the treatment groups, as compared to the control group. The treatment with SCO produced a significant reduction in the arm entries, as compared to control (P < 0.001, group: II vs. I). Further, the groups treated with

compounds **30**, **33** and donepezil also produced significant improvement in % novel arm entries as compared to SCO treatment (**Figure 5.10 (c)**).

5.3.8.1.4. Effect of scopolamine and various treatments on percentage total arm entries

SCO treatment indicated a significant reduction in total arm entries, as compared to the control group ($P < 0.05$, group: II vs. I). On the other hand, all the other treatment groups did not display any significant change with respect to the control as well as SCO treatment groups (**Figure 5.10 (d)**).

5.3.8.2. Barnes maze

5.3.8.2.1. Effect of scopolamine and various treatments on primary errors

The effect of treatment of SCO on the primary error was significantly high as compared to the control group ($P < 0.001$, group: II vs. I). The treatment with donepezil caused a significantly low primary error in the rats in comparison to SCO ($P < 0.001$, group III vs. II). Compound **30** displayed a significant reduction of primary error as compared to SCO ($P < 0.05$, group: IV vs II; $P < 0.01$, group: V vs II and $P < 0.001$, group: VII vs II). The compound also showed a significant reduction in primary error at all the doses in comparison to SCO ($P < 0.05$, group: VII vs II; $P < 0.05$, group: VIII vs II and $P < 0.001$, group: IX vs II). However, both the compounds did not display significant reduction in the primary error in a dose-dependent manner (**Figure 5.11 (a)**).

5.3.8.2.2. Effect of scopolamine and various treatments on primary latency time

SCO treatment caused a significant increase in the primary latency time, when compared with the control group ($P < 0.001$, group: II vs. I). There was a significant improvement in the latency period on the treatment with compound **30**, at all the doses as compared to SCO. The reduction in time was significant at 20 mg/Kg dose as compared to 5 mg/Kg for compound **30** ($P < 0.05$, group: VI vs. IV). Similarly, compound **33** also showed a significant reduction in primary latency time at all the doses. Compounds **30** and **33,** at a

dose of 20 mg/Kg, and donepezil displayed a significant decrease in primary latency time as compared to SCO ($P < 0.001$, groups: III vs. II, VI vs. II and IX vs. II) with no significant difference among each other (**Figure 5.11 (b)**).

5.3.8.3. Neurochemical analysis

5.3.8.3.1. Effect of scopolamine and various treatments on total ChE activity

The total ChE activity was determined for hippocampus and PFC regions with two different substrates, i.e., ATCI and BTCI. The total ChE activity of both the regions was found to be significantly elevated with ATCI as a substrate for SCO treatment in comparison to the control ($P < 0.001$, group: II vs I for both). Donepezil caused a significant reduction in enzymatic activity with ATCI as substrate as compared to SCO ($P < 0.001$, group: III vs. I). In case of hippocampus, all the selected doses, of both compounds **30** and **33,** displayed no significant difference when compared with SCO treatment. However, a significant difference was observed for all doses, of both the compounds, with donepezil treatment. On the other hand, the treatment with 10 and 20 mg/Kg doses of both compounds caused a significant reduction in the activity of enzymes as compared to SCO treatment ($P < 0.05$, groups: V vs. II, VI vs. II, VII vs. II and IX vs. II). While a dose of 5 mg/Kg of the compounds did not show significant difference in enzyme activity as compared to SCO, but a significant difference was observed when it was compared with donepezil treatment ($P < 0.05$, groups: IV vs. III and VII vs. III) (**Figure 5.12**).

The total ChE activity determined with BTCI as substrate also indicated a significant increase in enzymatic activity in hippocampus and PFC as compared to the control group ($P < 0.001$, group: II vs. I for both regions). In hippocampal samples, the treatment with compound **30** caused a significant reduction in ChE activity with BTCI as a substrate for doses of 10 and 20 mg/Kg ($P < 0.05$, groups: V vs. II, VI vs. II). Compound **33** also

produced a significant reduction in the total ChE activity at 20 mg/Kg dose in comparison to SCO ($P < 0.05$, group: IX vs. II). There was significant effect in the treatment groups of 5 mg/Kg for both compounds and 10 mg/Kg for compound **33**. Further, a dose of 5 mg/Kg of the two compounds did not display significant difference in the enzyme activity when compared with the SCO treatment in PFC.

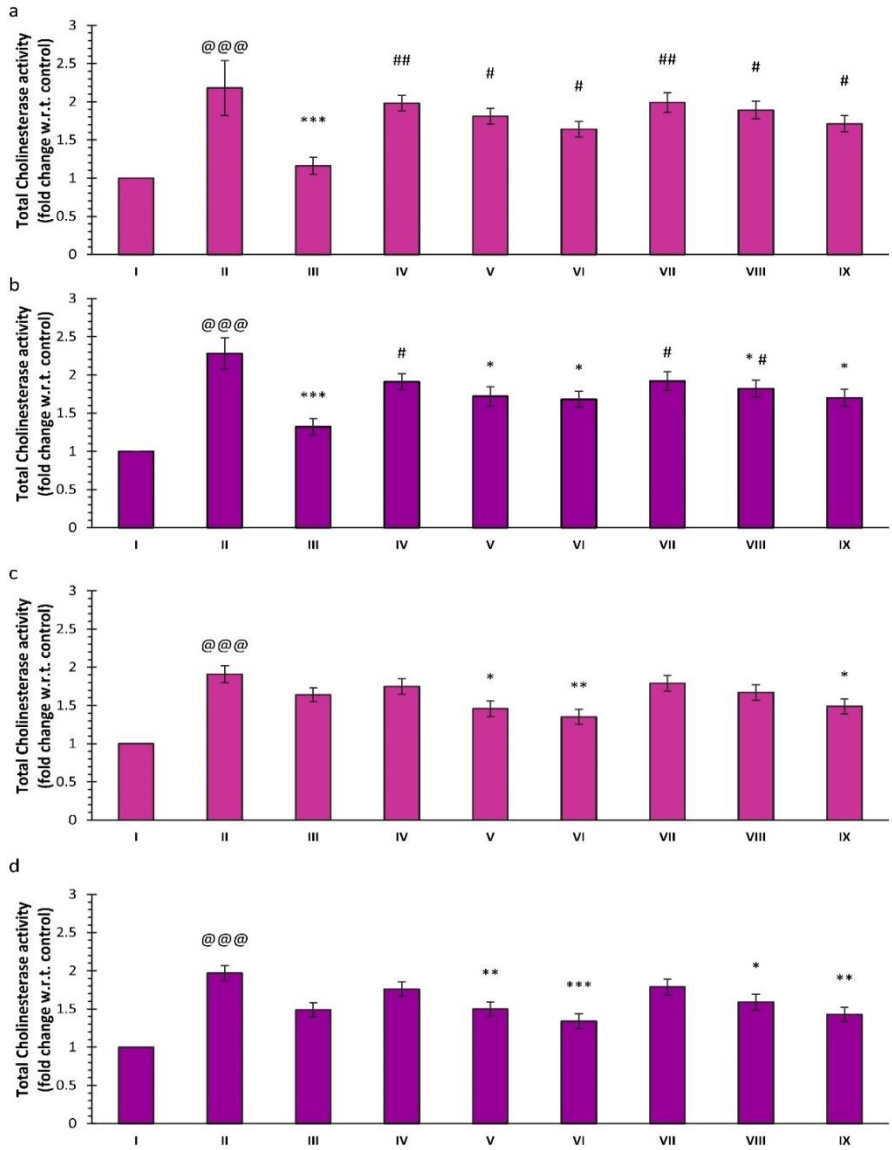

Figure 5.12 Effect of compounds **30, 33** and donepezil on total ChE activity with ATCI as substrate in (a) hippocampus, (b) PFC and with BTIC as substrate in (c) hippocampus, (d) PFC.

Data are expressed in Mean ± SEM (N =6, $^{@@@}$ $P < 0.001$ compared to control, * $P < 0.05$ compared to SCO, ** $P < 0.01$ compared to SCO, *** $P < 0.001$ compared to SCO, $^{\#}$ $P < 0.05$ compared to donepezil, $^{\#\#}$ $P < 0.01$ compared to donepezil, $^{\#\#\#}$ $P < 0.001$ compared to donepezil, $^{\wedge}$ $P < 0.05$ compared to compound **30**(5 mg/Kg), $^{\wedge\wedge}$ $P < 0.01$ compared to compound **30**(5 mg/Kg), $^{\wedge\wedge\wedge}$ $P < 0.001$ compared to compound **30**(5 mg/Kg), $^{\$}$ $P < 0.05$ compared to compound **33**(5 mg/Kg), $^{\$\$}$ $P < 0.01$ compared to compound **33**(5 mg/Kg) , $^{\$\$\$}$ $P < 0.001$ compared to compound **33**(5 mg/Kg)).

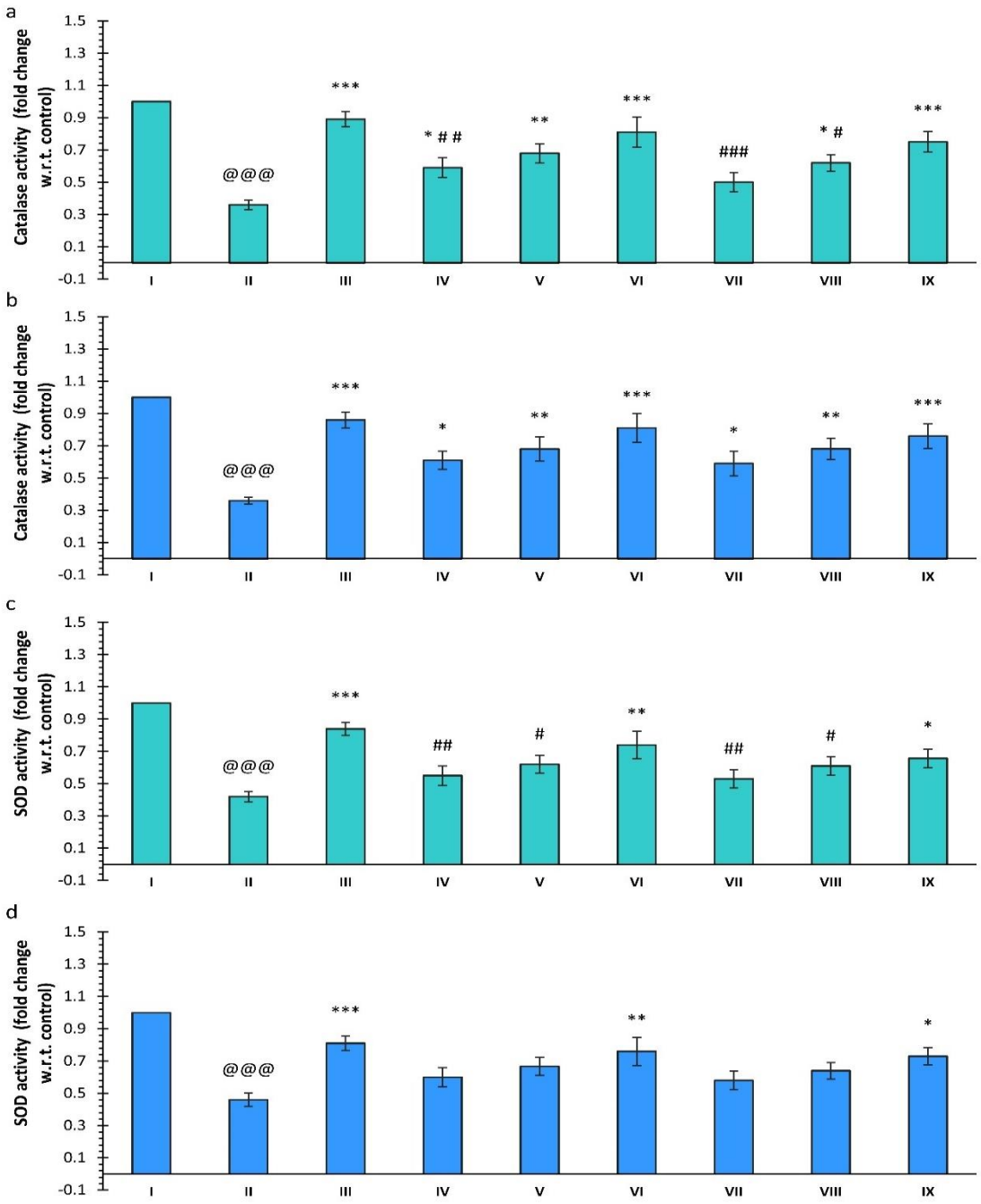

Figure 5.13 Effect of compounds **30, 33** and donepezil on CAT activity in (a) hippocampus, (b) PFC and SOD activity in (c) hippocampus, (d) PFC.

Data are expressed in Mean ± SEM (N =6, $^{@@@}$ P < 0.001 compared to control, * P < 0.05 compared to SCO, ** P < 0.01 compared to SCO, *** P < 0.001 compared to SCO, $^{\#}$ P < 0.05 compared to donepezil, $^{\#\#}$ P < 0.01 compared to donepezil, $^{\#\#\#}$ P < 0.001 compared to donepezil, $^{\wedge}$ P < 0.05 compared to compound **30**(5 mg/Kg), $^{\wedge\wedge}$ P < 0.01 compared to compound **30**(5 mg/Kg), $^{\wedge\wedge\wedge}$ P < 0.001 compared to compound **30**(5 mg/Kg), $^{\$}$ P < 0.05 compared to compound **33**(5 mg/Kg), $^{\$\$}$ P < 0.01 compared to compound **33**(5 mg/Kg) , $^{\$\$\$}$ P < 0.001 compared to compound **33**(5 mg/Kg))

The doses of 10 and 20 mg/Kg displayed a significant difference in enzymatic activity,

with BTCI as a substrate, when compared with the SCO in the PFC (P < 0.01, group: V

vs. II; P < 0.001, group: VI vs II; P < 0.05, group: VIII vs II and P < 0.01, group: IX vs. II).

5.3.8.3.2. Effect of scopolamine and various treatments on CAT activity

CAT activity was significantly reduced in the hippocampus and PFC regions of SCO treated group when compared to the control (P < 0.001, group: II vs. I). The treatment with donepezil caused significantly higher activity of the CAT in both the regions as compared to SCO treatment (P < 0.001, group: III vs. II). In the hippocampus region, it was observed that compound **30** produced a significant increase in CAT activity for all the doses with the maximum activity observed at 20 mg/Kg dose (P < 0.05, group: IV vs. II; P < 0.01, group: V vs. II and P < 0.001, group: VI vs II). The treatment with compound **33** showed significant improvement in the levels of CAT activity at 10 and 20 mg/Kg doses (P < 0.05, group: VIII vs. II and P < 0.001, group: IX vs. II). The CAT activity of the PFC region was also found to be significantly high for all the doses of compounds **30** and **33** when compared to SCO (**Figure 5.13**).

5.3.8.3.3. Effect of scopolamine and various treatments on SOD activity

The treatment of SCO resulted in a significant decrease in SOD activity in both hippocampus and PFC, when compared to the control (P < 0.001, group: II vs. I). In case of donepezil, SOD level was significantly high in both regions as compared to SCO treatment (P < 0.001, group: III vs. II). The treatment of compounds **30** and **33** at a dose of 20 mg/Kg showed significantly high SOD activity as compared to SCO (P < 0.01, group: VI vs. II and P < 0.05, group: IX vs II) in the hippocampal region. The other doses did not produce any significant increase in SOD activity. In the case of PFC, it was also found that a dose of 20 mg/Kg of the two compounds displayed the significant higher activity of SOD as compared to SCO treatment (P < 0.01, group: VI vs. II and P < 0.05, group: IX vs II) (**Figure 5.13**).

5.3.8.4. Biochemical analysis

There was no significant difference in the levels of SGPT and SGOT enzymes between the control and the treatment groups in biochemical analysis. Similarly, no significant difference was observed in serum creatinine and urea levels among the control and the treatment groups (**Figure 5.14**).

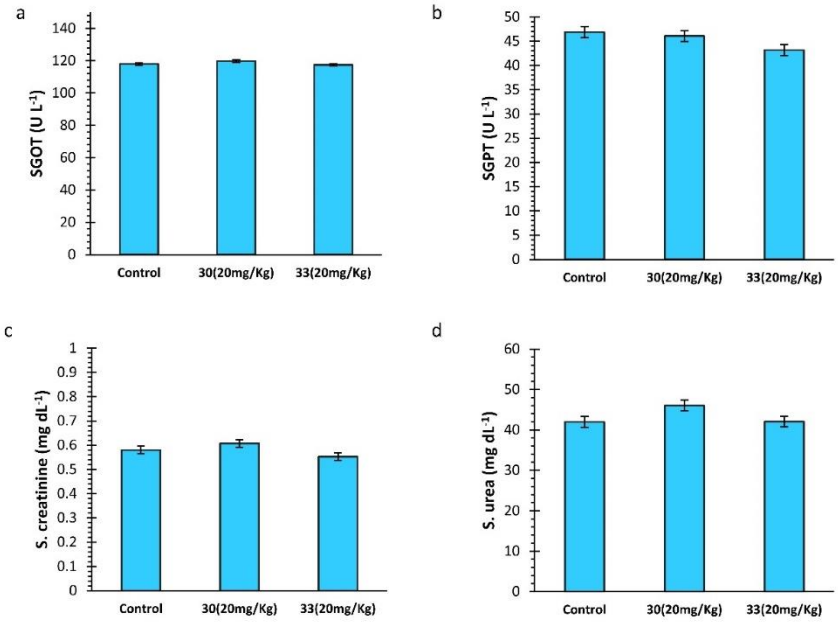

Figure 5.14 Effect of compounds **30** and **33** on (a) SGOT, (b) SGPT, (c) S. creatinine and (d) S. urea levels. Data are expressed in Mean ± SEM (N =6).